Atmos. Chem. Phys. Discuss., 15, 33331–33378, 2015
www.atmos-chem-phys-discuss.net/15/33331/2015/
doi:10.5194/acpd-15-33331-2015


Atmospheric Chemistry and Physics Discussions



# Vertical and horizontal variability of $PM_{10}$ source contributions in Barcelona during SAPUSS

**M. Brines[1,2], M. Dall'Osto[3], F. Amato[1], M. C. Minguillón[1], A. Karanasiou[1], A. Alastuey[1], and X. Querol[1]**

[1]Institute of Environmental Assessment and Water Research (IDÆA) Consejo Superior de Investigaciones Científicas (CSIC), C/Jordi Girona 18-26, 08 034 Barcelona, Spain
[2]Department of Astronomy and Meteorology, Faculty of Physics, University of Barcelona, C/Martí i Franquès 1, 08 028 Barcelona, Spain
[3]Institute of Marine Sciences (ICM) Consejo Superior de Investigaciones Científicas (CSIC), Pg. Marítim de la Barceloneta 37-49, 08 003 Barcelona, Spain

Received: 2 November 2015 – Accepted: 3 November 2015 – Published: 26 November 2015

Correspondence to: M. Brines (mariola.brines@idaea.csic.es)

Published by Copernicus Publications on behalf of the European Geosciences Union.







## Abstract

During the SAPUSS campaign (Solving Aerosol Problems by Using Synergistic Strategies) $PM_{10}$ samples at twelve hours resolution were simultaneously collected at four monitoring sites located in the urban agglomerate of Barcelona (Spain). A total of 221 samples were collected from 20 September to 20 October 2010. The Road Site (RS) site and the Urban Background (UB) site were located at street level, whereas the Torre Mapfre (TM) and the Torre Collserola (TC) sites were located at 150 m a.s.l. by the sea side within the urban area and at 415 m a.s.l. 8 km inland, respectively. For the first time, we are able to report simultaneous $PM_{10}$ aerosol measurements allowing us to study aerosol gradients at both horizontal and vertical levels. The complete chemical composition of $PM_{10}$ was determined on the 221 samples, and factor analysis (Positive Matrix Factorisation, PMF) was applied. This resulted in eight factors which were attributed to eight main aerosol sources affecting $PM_{10}$ concentrations in the studied urban environment: (1) vehicle exhaust and wear (2–9 $\mu g\,m^{-3}$, 10–27 % of $PM_{10}$ mass on average), (2) road dust (2–4 $\mu g\,m^{-3}$, 8–12 %), (3) mineral dust (5 $\mu g\,m^{-3}$, 13–26 %), (4) aged marine (3–5 $\mu g\,m^{-3}$, 13–20 %), (5) heavy oil (0.4–0.6 $\mu g\,m^{-3}$, 2 %), (6) industrial (1 $\mu g\,m^{-3}$, 3–5 %), (7) sulphate (3–4 $\mu g\,m^{-3}$, 11–17 %) and (8) nitrate (4–6 $\mu g\,m^{-3}$, 17–21 %). Three aerosol sources were found enhanced at the ground levels (confined within the urban ground levels of the city) relative to the upper levels: (1) vehicle exhaust and wear (2.8 higher), (2) road dust (1.8 higher) and (3) local urban industries/crafts workshops (1.6 higher). Surprisingly, the other aerosol sources were relatively homogeneous at both horizontal and vertical levels. However, air mass origin and meteorological parameters also played a key role in influencing the variability of the factors concentrations. The mineral dust and aged marine factors were found to be a mixture of natural and anthropogenic components and were thus further investigated. Overall, three types of dust were identified to affect the urban study area: road dust (35 % of the mineral dust load, 2–4 $\mu g\,m^{-3}$ on average), Saharan dust (28 %, 2.1 $\mu g\,m^{-3}$) and background mineral dust (37 %, 2.8 $\mu g\,m^{-3}$). Our results evidence that






ACPD
15, 33331–33378, 2015



although the city of Barcelona broadly shows a homogeneous distribution of $PM_{10}$ pollution sources, non-exhaust traffic, exhaust traffic and local urban industrial activities are major coarse $PM_{10}$ aerosol sources.

## 1 Introduction

The study of ambient particulate matter (PM) concentrations in urban environments is of particular interest due to its adverse effects on human health (Pope and Dockery, 2006; Pope et al., 2009; Lim et al., 2012). However, the identification and quantification of PM sources – the basis for the design of mitigation strategies – remains challenging due to their complex nature. Indeed, aerosols have multiple sources, and emissions from the same source will change with time and operating conditions. Source apportionment of airborne particulate matter has assumed increasing importance in recent years (Viana et al., 2008; Beddows et al., 2015). This is because current legislation has highlighted the need for reliable quantitative knowledge of the source apportionment of particulate matter in order to devise cost-effective abatement strategies. To apportion PM sources, many tools have been used for their identification and quantification (Viana et al., 2008). Chemical speciation of ambient PM coupled to receptor modelling is currently considered one of the most powerful tools for this purpose (Srimuruganandam and Shiva Nagendra, 2012; Waked et al., 2014). Within factor analytical models, the positive matrix factorization (PMF) one is highly recommended when sources are not formally known (Paatero and Tapper, 1994). PMF has been used in many studies dealing with air pollution in urban areas in America, Europe, and Asia. Many sources such as road transport, industrial emissions, sea salt, and crustal dust were identified using this method (Viana et al., 2008). Apportioning correctly the sources of airborne particulate matter is important because there are most probably differences in the toxicity of particles according to their chemical composition. In other words, PM from different sources may have a very different potency in affecting human health (Kelly and Fussell, 2012).





ACPD
15, 33331–33378, 2015



Urban $PM_{10}$ concentrations show significant variability across Europe. In northern European countries, the road dust originated by pavement abrasion due to the use of studded tires (Norman and Johansson, 2006), high sea salt concentrations in the coastal areas (Yin et al., 2005) and the use of biomass burning for heating purposes are significant sources of PM (Puxbaum et al., 2007). By contrast, in southern European countries – due to the drier climate conditions – mineral dust, resuspension and Saharan dust outbreaks substantially contribute to PM concentrations (Putaud et al., 2010; Kassomenos et al., 2014; Amato et al., 2015). Broadly, the elevated concentrations usually observed in Southern Europe are attributed to the combination of diverse emission sources including industry, traffic, resuspended dust, shipping emissions and African dust outbreaks. Recently, a huge effort has been made in assessing the PM trends in the Mediterranean basin, including the MED-PARTICLES project (Karanasiou et al., 2014) and the AIRUSE LIFE project (Amato et al., 2015). It is important to remember that most of the PM urban studies are based on ambient measurements taken at a single sampling point in a city, but the pollutants concentrations may vary across the city. On this regard it is worth reporting the studies of the ESCAPE project (Eeftens et al., 2012) which aimed to investigate long-term effects on human health of exposure to air pollution in Europe, and showed large spatial variability of trace elements and sources for improved exposure assessment (Minguillon et al., 2014).

The work presented in this manuscript is part of the FP7-PEOPLE-2009-IEF SAPUSS project (Solving Aerosol Problem by Using Synergistic Strategies), where for the first time in the Mediterranean basin both the spatial vertical and horizontal distributions of air pollutants were investigated (Dall'Osto et al., 2013a). SAPUSS allows to better understand the complex interactions between these pollutants and different meteorological variables, as well as their influence on air quality. As reported by Han et al. (2015), with the increase of vertical height the influence of source emissions on local air quality is weakening, but the characteristics of regional pollution gradually become obvious. The novelty of SAPUSS relies in the fact that by simultaneously measuring across the vertical and horizontal urban scale, local and regional PM sources





ACPD
15, 33331–33378, 2015



can be better apportioned. Unfortunately, there are very few studies conducted in European urban vertical columns specifically looking at chemically resolved aerosol sources (Ferrero et al., 2010, 2014; Harrison et al., 2012; Curci et al., 2015). A larger number of aerosol vertical studies is found in Asia, perhaps because a larger number of people live in high-rise buildings. For example, an estimated 57.7 % of the 6.5 million residents in the Taipei metropolis lived on or above the third story (Wu and Lung, 2012). Most studies of vertical gradients of PM in urban environments consisted of a tower with aerosol and meteorological instrumentation deployed at different levels, up to 320 m (Chan et al., 2005; Tao et al., 2007; Zhang et al., 2011; Shi et al., 2012; Xiao et al., 2012; Öztürk et al., 2013; Sun et al., 2013; Tian et al., 2013; Moeinaddini et al., 2014; Wu et al., 2014). Higher concentrations of primary emitted contaminants were found at the lower levels, reflecting the closeness to the emission sources (Tian et al., 2013). However, at some sites high PM concentrations were recorded at the top level due to long-range transport of secondary pollutants (Harrison et al., 2012; Shi et al., 2012; Xiao et al., 2012; Sun et al., 2013; Moeinaddini et al., 2014).

Atmospheric aerosol characteristics in the city of Barcelona and its surrounding area have been studied in great detail. The main sources of $PM_{10}$ are mineral dust sources and road traffic emissions (Amato et al., 2009; Pérez et al., 2010). Other minor sources comprise shipping, both due to the city harbour and regional sources in the Mediterranean Basin (Querol et al., 2009; Pey et al., 2010). Industry represents usually less than 10 % of $PM_{10}$ mass, being V and Ni common tracers both for shipping and industrial activities (Querol et al., 2009; Viana et al., 2014). Biomass burning contribution to $PM_{10}$ is relatively low in the study area (Minguillón et al., 2011; Reche et al., 2012). Secondary aerosol components affect $PM_{10}$ especially during regional recirculation episodes, were the stagnant conditions lead to the accumulation of pollutants (Pandolfi et al., 2014). In addition, due to the coastal location of the study area, sea breeze (during the day) and mountain breeze (during the night) also influence pollution transport from/towards the urban area. However, the urban vertical column of Barcelona – and other Mediterranean cities – are not characterised at all. Within the scope introduced in





ACPD
15, 33331–33378, 2015



the presenting overview paper of this special issue (Dall'Osto et al., 2013a), the main objective of this work are:

- to interpret the variability of aerosol levels and composition in the urban Mediterranean environment of Barcelona, the second largest city in Spain and a major metropolitan agglomerate in Europe.
- To study aerosol particle mass in terms of the sources and the physico-chemical transformations occurring simultaneously at the road, background, tower and regional background sites.
- To apply receptor modelling to $PM_{10}$ organic and inorganic species, in order to allow the identification of emission sources and their respective contributions to the PM mass in ambient air.

Our unique approach relies in the fact that – for the first time – both horizontal and vertical $PM_{10}$ measurements were taken simultaneously in four different sites across the urban agglomerate of Barcelona. Special emphasis is given in describing gradients ground/tower and the variability of each factor concentrations under different air masses.

## 2 Methodology

### 2.1 Location

Measurements were performed in the urban agglomerate of Barcelona, a city located in the NE of Spain in the Western Mediterranean Basin (WMB). It is geographically constrained by the Llobregat and Besòs valleys (to the SW and NE, respectively) and the coastal range of Collserola to the N. The city has a population of 1.7 million, and the metropolitan area exceeds 4 million. These conditions result in a highly populous urban area and one of the highest car densities in Europe (6100 cars $km^{-2}$, DGT 2015). More





ACPD
15, 33331–33378, 2015



detailed information about the SAPUSS study area can be found elsewhere (Dall'Osto et al., 2013a). The structure of the planetary boundary layer (PBL) above Barcelona was monitored by simultaneous measurements of ceilometers (Pandolfi et al., 2013). The field campaign took place in Barcelona from 20 September to 20 October 2010, including six sampling sites (Dall'Osto et al., 2013a). From those, the following four monitoring sites are considered for the present study:

- Road Site (RS): it represents the average conditions of a trafficked road in the city centre (about 17 000 vehicles per day). The monitoring site was located in the Urgell Street, a street canyon with four vehicle lanes (one direction) and cycling lanes in both directions.
- Urban Background (UB): it represents the urban background environment of Barcelona. It is located NW of the city centre in a small park 300 m away from the busy Diagonal Avenue, a nine-lanes road used primarily by commuters (62 000 vehicles per day).
- Torre Mapfre (TM): it is a skyscraper located 300 m from the coast in the Olympic Port of Barcelona, close to a recreational harbour and leisure area. There is a tunnelled motorway ring road (four lanes) at 50 m distance from the building and two three-lanes roads at ground level. The measurements were taken at the rooftop terrace of the tower (150 m a.s.l.).
- Torre Collserola (TC): this site was found at the Fabra Observatory (415 m a.s.l.), about 450 m from the Collserola tower (TC), where additional instrumentation was deployed (see Dall'Osto et al., 2013a). Due to logistical reasons at the TC site (limited access and storage space), the Fabra Observatory ($TC_g$) was used as a monitoring site for the $PM_{10}$ aerosol chemical measurements. In this study the $TC_g$ is named TC for simplicity. Measurements in this monitoring site were taken at ground level (10 m above ground) but at an overall height of 425 m a.s.l.





ACPD
15, 33331–33378, 2015



It is important to note that whilst TM is well within the Barcelona urban city centre, TC is located in the hills of the urban background of Barcelona. It is worthwhile to stress that the two monitoring towers are the tallest buildings within several kilometres of the sites, with good exposure to winds from all directions (Dall'Osto et al., 2013a). The mean ceilometer surface mixed layer (SML) and decoupled residual/convective layer (DRCL) heights over the whole SAPUSS campaign were found to be 904 ± 273 m a.g.l. and 1761 ± 363 m a.g.l., respectively (Pandolfi et al., 2013), all well above all the four measurements sites described in this study. PBL maximum height ($H$) and daily variations (DV) were strongly dependent on air mass types, ranging from the highest $H$ – strongest DV during the Atlantic air masses to the lowest $H$ – weakest DV during the North African air masses, but overall always above both measurements towers and other monitoring sites.

### 2.2 Measurements

High volume samplers DIGITEL DHA-80 and MCV CAV-A/mSb (30 $m^3 h^{-1}$) equipped with $PM_{10}$ heads collected 12 h samples (from 11:00 to 23:00 and from 23:00 to 11:00, local time) on quartz fibre filters (Pallflex 2500QAT-UP) at the four monitoring sites. A total of 221 filter samples were collected, from which 93 % were collected simultaneously at the four monitoring sites (54 concurrent samples per site).

Meteorological parameters (temperature, relative humidity, wind speed and direction, solar radiation and pressure) were measured at the same sampling sites or at the nearest available meteorological station, as described elsewhere (Dall'Osto et al., 2013a).

#### 2.2.1 PM concentration and chemical composition

$PM_{10}$ mass concentrations were determined gravimetrically. The samples were analysed following the methodology described by Querol et al. (2001). Briefly, a quarter of the filter was acid digested ($HNO_3 : HF : HClO_4$), and the resulting solution was an-





ACPD
15, 33331–33378, 2015



alyzed for Al, Ca, K, Mg, Fe, Ti, Mn, P, S, Na and 25 trace elements by inductively coupled plasma atomic emission and mass spectrometry (ICP-AES and ICP-MS), respectively; a quarter of the filter was water-extracted and the concentrations of $SO_4^{2-}$, $NO_3^-$ and $Cl^-$, and $NH_4^+$ were determined by ion chromatography (IC) and selective electrode, respectively. A section of 1.5 $cm^2$ of the filter was used to determine organic carbon (OC) and elemental carbon (EC) by a thermal–optical transmission technique (Birch and Cary, 1996) using a Sunset Laboratory OCEC Analyzer following the EUSAAR2 temperature protocol (Cavalli et al., 2010). Laboratory and field blanks were analysed following the same procedure. Ambient concentrations were calculated based on the samples and the blanks concentrations.

Crustal and sea salt aerosols concentration were also estimated. Moreno et al. (2006) reported the average composition of mineral dust originated in the North African region that later reached the WMB. Based on the average Na/Al ratio of the North African dust, the mineral Na (or non-sea salt Na, nss Na) can be calculated from the Al concentrations, hence the remaining Na is attributed to sea salt (ss Na). The sea salt load for each sample was calculated based on the ss Na and the standard sea salt composition which includes Na, $Cl^-$, ss Mg, ss Ca and ss $SO_4^{2-}$ (Mészáros, 1999).

Mineral matter was then calculated as the sum of $SiO_2$, $CO_3^{2-}$, $Al_2O_3$, nss Ca, Fe, K, nss Mg and nss Na. $SiO_2$ concentrations were estimated as $3 \times Al_2O_3$. $CO_3^{2-}$ concentrations were estimated as $1.5 \times Ca$, assuming that all Ca is present as $Ca(CO_3)_2$ (Karanasiou et al., 2011). Organic matter (OM) was estimated as OC multiplied by a factor 1.4 at the RS, 1.6 at the UB and TM and 2.1 at the TC, according to Turpin and Lim (2001).

### 2.2.2 Source apportionment

A constrained Positive Matrix Factorization (PMF, Paatero and Tapper, 1994) model was applied using the Multilinear Engine (ME-2) (Paatero, 1999) to assess the source apportionment.





ACPD
15, 33331–33378, 2015



PMF is a widely used receptor model based on the mass conservation principle:

$$x_{ij} = \sum_{k=1}^{p} g_{ik} f_{jk} + e_{ij} \quad i = 1,2,\ldots,m \quad j = 1,2,\ldots,n \tag{1}$$

where $x_{ij}$ is the $i$th concentration of the species $j$, $g_{ik}$ is the $i$th contribution of the source $k$ and $f_{jk}$ is the concentration of the species $j$ in source $k$, and $e_{ij}$ are the residuals. Equation (1) can be also expressed in matrix form as $\mathbf{X} = \mathbf{G}\mathbf{F}^T + \mathbf{E}$. PMF solves Eq. (1) minimizing the object function $Q$:

$$Q = \sum_{i=1}^{n} \sum_{j=1}^{m} (e_{ij}/s_{ij})^2 \tag{2}$$

where $s_{ij}$ are the individual data uncertainties. The uncertainty estimates were based on the approach by Escrig Vidal et al. (2009) and Amato et al. (2009) and provided a criterion to separate the species which retain a significant signal from the ones dominated by noise. This criterion is based on the signal-to-noise $S/N$ ratio defined by Paatero and Hopke (2003). Species with $S/N < 2$ are generally defined as weak variables and downweighted by a factor of 3. Nevertheless, since $S/N$ is very sensitive to sporadic values much higher than the level of noise, the percentage of data above detection limit was used as complementary criterion. All the samples collected at the four sites were gathered in one data matrix. This data assembling allows exploring a larger area of the $N$-dimensional source contributions space. The data matrix was uncensored, i.e. negative, zero and below detection limit values were included as such in the analyses to avoid a bias in the results (Paatero, 2007). A total of 221 samples containing 32 different species were included in the PMF which was run by means of the Multilinear Engine-2 program allowing to handle a priori information as shown in the Results section. A bootstrap technique was used to estimate the uncertainties of factor profiles, based on the EPA PMF v3.0 script. It consisted on three different steps: re-sampling, reweighting and random rotational pulling (Tukey, 1958; Efron and Tibshirani, 1986).





ACPD
15, 33331–33378, 2015



A seed value of 7 was used with 20 runs. Rotational ambiguity was reduced by means of the implementations of the constraints and evaluated through bootstrapping. The final number of factors was chosen based on several criteria: *Q* values, factors profiles and contributions, distribution of scaled residuals and *G* space plots.

## 3 Results

### 3.1 $PM_{10}$ concentration and chemical composition in a three dimension (3-D) scenario

As presented in the introduction overview paper of this special issue (Dall'Osto et al., 2013a), the average $PM_{10}$ concentrations at the four monitoring sites during SAPUSS followed a decreasing trend from the site closest to traffic sources to the one located in the suburban background at 415 m a.s.l. (RS 30.7, UB 25.9, TM 24.8 and 21.8 $\mu g\,m^{-3}$ at TC; Table 1). This suggests that the city surface is enhanced in coarse particles. It is important to note that the high $PM_1/PM_{10}$ ratios at the towers (TM, TC) are not only due to the low $PM_{10}$ concentrations, as the absolute values of $PM_1$ detected at the tower sites were also higher than the urban background ground levels. Deng et al. (2015) recently also reported that – overall – the vertical distributions of $PM_{10}$, $PM_{2.5}$, and $PM_1$ decreased with height. The lapse rates showed the following sequence: $PM_{10} > PM_{2.5} > PM_1$, which indicates that the vertical distribution of fine particles is more uniform than that of coarse particles; and the vertical distribution in summer is more uniform than in other seasons.

Whilst the chemical analysis of the PM mass was only briefly described in an earlier study (Dall'Osto et al., 2013a), in this section the chemical components building up the $PM_{10}$ mass concentrations are described in more details. The major $PM_{10}$ components are summarised in Table 1, whereas the concentrations of each analysed species is shown in Table S1 in the Supplement. Figures 2 and 3 show the absolute and relative contributions to $PM_{10}$ at each site. Briefly:





ACPD
15, 33331–33378, 2015



– crustal elements accounted for 14–17 % of the mass, suggesting an unexpectedly homogeneous relative contribution to the total $PM_{10}$ across the Barcelona urban area (Table 1, Fig. 2). However, absolute mass concentrations of crustal matter (Fig. 3a) decreased from the city centre sites (5.2 $\mu g\,m^{-3}$ at RS) to those located further inland (3.1 $\mu g\,m^{-3}$ at TC), suggesting higher contribution of dust in the lower level monitoring sites.

– Sea salt aerosols relative contribution was homogenous at all sites ranging from 7–11 % (1.5–2.7 $\mu g\,m^{-3}$, Table 1, Fig. 2). Figure 3b shows that the highest concentrations were recorded near the sea side monitoring sites (TM, RS), with a decreasing gradient recorded towards inland (UB, TC). Despite TM being located a few meters from the sea side, it shows similar concentrations to RS, 4 km distant. This might be due to the elevation of the TM sampling site (150 m a.s.l.) causing dilution of surface sea spray.

– Secondary inorganic aerosols (SIA: sulphate $SO_4^{2-}$, nitrate $NO_3^-$ and ammonium $NH_4^+$) display altogether similar concentrations at the city sites (6.3 $\mu g\,m^{-3}$ on average at RS, 5.7 $\mu g\,m^{-3}$ at UB and 5.8 $\mu g\,m^{-3}$ at TM) and decrease around 25 % at TC (4.4 $\mu g\,m^{-3}$). Overall, SIA accounted for 20–23 % of the mass (4.4–6.3 $\mu g\,m^{-3}$, see Fig. 2). The contribution of ammonium was similar at all sites, around 2–3 % (0.5–0.9 $\mu g\,m^{-3}$) of $PM_{10}$ mass. Sulphate and nitrate contributed in similar proportions at all sites, ranging from 7–11 % each (1.6–2.6 $\mu g\,m^{-3}$ for nitrate and 2.3–2.8 $\mu g\,m^{-3}$ for sulphate), although in absolute concentrations a decrease of 15–35 % at the TC was detected for SIA (see Fig. 3c).

– Elemental carbon (EC) concentration was clearly influenced by traffic sources, as its contribution decreased with the distance to traffic hot spots (RS: 1.4 $\mu g\,m^{-3}$, 5 %; UB: 0.9 $\mu g\,m^{-3}$, 3 %; TM: 0.7 $\mu g\,m^{-3}$, 3 %; TC: 0.5 $\mu g\,m^{-3}$, 2 % – see Figs. 2 and 3d).





ACPD
15, 33331–33378, 2015



– Organic matter (OM) accounted for 16–21 % of the mass and was found in the highest relative proportion at the TC site due to its location on a nearby hill in a suburban environment. The lowest concentrations were observed at UB and TM (4.2 $\mu g\,m^{-3}$), followed by TC (4.6 $\mu g\,m^{-3}$), while the highest ones were recorded at the RS (5.2 $\mu g\,m^{-3}$ – see Figs. 2 and 3d).

– The unaccounted mass of PM (31–35 %) is that resulting from the difference of the gravimetric measurements of the filters and the sum of all the components determined by chemical analysis. This unaccounted mass is usually attributed to water molecules contained in potential remaining moisture, and crystallisation and formation water (water molecules in the structure of specific chemical species), as well as heteroatoms contained in the organic species and not analysed (Querol et el., 2001; Amato et al., 2015).

Despite the low contribution of trace elements to the bulk $PM_{10}$ (< 1 %), their concentrations provide valuable information by tracing specific pollution sources. Figure 3e–j show the concentration of a selection of trace elements associated with four known sources affecting the metropolitan area of Barcelona: crustal, road traffic, industry and shipping. The most abundant crustal tracer is Ti followed by far by Rb, Y, Ce, La, Li, Nd, and Ga. Such elements were found in higher concentrations at the ground sites (RS and UB) relative to the tower sites (TM and TC). This might be due to the dust resuspension by road traffic or other anthropogenic sources such as construction works or parks, thus producing a vertical decreasing gradient. The spatial variability of vehicle wear tracers such as (Cu, Sn and Ba; Schauer et al., 2006) is driven by the proximity to traffic sources, being the RS the most polluted site. The industrial emissions tracers for the city of Barcelona (Zn, Mn, Pb, As and Ni; Amato et al., 2009) showed higher concentrations at the UB followed by the RS, TM and TC. This is likely to be due to the pollution plumes originating from the industrial area along the Llobregat Basin (south-western side of Barcelona metropolitan area) that first impacts the UB site (Dall'Osto et al., 2013b). On the other hand, the remaining industrial tracers Cu and Sb (show-





ACPD
15, 33331–33378, 2015



ing a decreasing gradient with the distance to traffic sources) might account for both industrial and traffic-related emissions. Both traffic and industrial tracers showed significant higher values at the ground sites respect the tower sites. On this regards, it is worth to remember that V and Ni (Fig. 3i–j) are usually associated with shipping emissions (Kim et al., 2008; Agrawal et al., 2008). Indeed, higher V levels were found at the sites closer to the coast (TM and RS), in agreement with findings from Minguillón et al. (2014). However, higher Ni concentrations were recorded at the ground sites (UB and RS) respect to the tower sites (TM and TC), probably due to the contribution of other Ni sources reaching the ground sites (e.g. smelters). Viana et al. (2014) reported a V/Ni ratio associated to shipping emissions of 2.3–4.5. In our study the only site within this range was TM (2.4), located closest to the sea side. RS and UB showed lower ratios (1.3 and 1.1, respectively) probably due to the higher impact of an industrial plume containing Ni. TC ratio was 2.0, which might indicate an additional V loading of crustal origin, due to its location on a nearby hill.

### 3.2 Source apportionment and temporal variability in a 3-D scenario

The PMF analysis was applied to the $PM_{10}$ data matrix, which contained 221 samples (56 at RS, 54 at UB, 55 at TM and 56 at TC). The method herein used is the same of the one recently reported by Amato et al. (2015), aiming at characterising similarities and heterogeneities in PM sources and contributions in urban areas from Southern Europe. This method is not new, as it was already proven to increase considerably the statistical significance of the analysis (Amato et al., 2009). Different constraints were added into the PMF model (Paatero and Hopke, 2008), in order to reduce rotational ambiguity. The PMF solution chosen was an eight factor solution, with a $Q$ (constrained) value of 6627, being the $Q/Q_{exp}$ ratio 1.17, and with an increase d$Q$ of 7.5 % with respect to the base run, due to the implementation of auxiliary equations. One factor (road dust) was pulled towards the composition of local road dust (average of city centre samples, as reported by Amato et al., 2009). The Na/Al ration pulled towards the value reported for earth's crust composition by Mason (1966) in form of auxiliary equations (Paatero and





ACPD
15, 33331–33378, 2015



Hopke, 2009). Overall, a total of eight factors were identified by the application of PMF: (1) "vehicle exhaust and wear", (2) "road dust", (3) "mineral", (4) "aged marine", (5) "heavy oil", (6) "industrial", (7) "sulphate" and (8) "nitrate". The average concentrations of each factor registered at each site are shown in Fig. 5 and Table 2, while Fig. S1 in the Supplement displays the temporal variation of each factor for all sites. To further complete the analysis and interpretation of the results, Polar Plots were obtained using the OPENAIR software package of R (Carslaw and Ropkins, 2012; R Development Core Team, 2012). These plots display the different factors concentrations depending on the blowing wind direction and speed, thus allowing deducing the main pollution sources origin (Fig. S2). The eight identified aerosol PMF factors characteristics can be seen in Fig. 4 and are summarised as:

- the vehicle exhaust and wear factor profile (Fig. 4a) was dominated by EC and OC originating from vehicle exhaust emissions. Other chemical elements include Cu, Sb, Cr, Fe and Sn (67, 53, 46, 41 and 39 % of the variation, respectively) which are usually present in the brake and tyre wear (Sternbeck et al., 2002; Ntziachristos et al., 2007; Amato et al., 2009). Due to its direct traffic origin, this factor accounts for the highest mass contribution at the RS (27 %, 8.7 $\mu g\,m^{-3}$), followed by UB (18 %, 5.0 $\mu g\,m^{-3}$), TM (11 %, 2.9 $\mu g\,m^{-3}$) and TC (10 %, 1.9 $\mu g\,m^{-3}$) (see Table 2 and Fig. 4a). A clear horizontal and vertical gradients can be seen for the $PM_{10}$ contributions of this source. It originated at the traffic hot spots near RS, UB and TM and was later transported upslope towards TC by the sea breeze, where the maximum concentrations were recorded under SE winds from the city (Fig. S2).

- The road dust PMF factor profile (Fig. 4b) was constrained using the emission profile reported for the city of Barcelona by Amato et al. (2009) by means of a pulling equation. It contained high concentrations of $Al_2O_3$, Ca, Fe, Li, Ti but also explained around 20 % of the variation of Cu and Sb (Table 2 and Fig. 4b). As expected, this factor concentration followed also a decreasing trend from RS (12 %, 3.8 $\mu g\,m^{-3}$) and UB (12 %, 3.3 $\mu g\,m^{-3}$) to TM (8 %, 2.3 $\mu g\,m^{-3}$) and TC





ACPD
15, 33331–33378, 2015



(9 %, 1.6 $\mu g\,m^{-3}$). The road dust was transported from the nearby busy streets towards the sites, as seen in Fig. S2.

– The mineral PMF factor profile (Fig. 4c) was mainly made up of $Al_2O_3$, Ti, Rb, La, Li and Se (42, 45, 36, 27, 26, 22 % of the variation, respectively). Unexpectedly, average absolute concentrations were very homogeneous across the city (4.6 to 5.1 $\mu g\,m^{-3}$, 13–26 %) pointing to a source affecting the whole urban area.

– The aged marine PMF factor profile (Fig. 4d) contribution is characterised by Na and Cl (75 and 52 % of the variation, respectively) and also a proportion of Mg and $SO_4^{2-}$ (48 and 22 % of the variation, respectively). The ratio $SO_4^{2-}$/Na exceeded the calculated sea salt ratio, indicating its aged nature. As expected, the highest concentrations were reached at the sites located closer to the sea (TM, 20 %, 5.2 $\mu g\,m^{-3}$; RS, 14 %, 4.6 $\mu g\,m^{-3}$; UB, 13 %, 3.6 $\mu g\,m^{-3}$; TC, 13 %, 2.6 $\mu g\,m^{-3}$). The highest concentrations at all sites were reached under E-SE blowing winds (caused by sea breeze, Fig. S2).

– The heavy oil PMF factor profile (Fig. 4e) was characterized by V and Ni (71 and 45 % of the variation, respectively) and showed a relevant concentration of $SO_4^{2-}$ and EC. It was attributed to fuel oil combustion from shipping emissions since power generation around Barcelona is only allowed by using natural gas since 2008. Furthermore, 98 % of domestic heating systems use natural gas, and the spatial distribution of V concentrations evidenced higher levels as we approach the coast (Table S1). Average concentrations varied between 0.4–0.6 $\mu g\,m^{-3}$, representing on average about 2 % of the load at each site (Table 2).

– The industrial PMF factor profile (Fig. 4f) was defined by Pb, Zn, Mn and Cd (50, 44, 31 and 19 % of the variation, respectively). It was related to the smelters and cement kilns located along the nearby Llobregat valley, NW of the city (Amato et al., 2009; Moreno et al., 2011; Dall'Osto et al., 2013b). The emission plume was transported towards the city by the night land breeze (Fig. S2), reaching the





ACPD
15, 33331–33378, 2015



ground sites UB and RS in a greater measure due to proximity of the sources (RS, 4 %, 1.2 µg m$^{-3}$; UB, 5 %, 1.4 µg m$^{-3}$; TM, 3 %, 0.7 µg m$^{-3}$; TC, 4 %, 0.9 µg m$^{-3}$). The highest peaks (6–8 µg m$^{-3}$) were recorded for the UB site the 5 October and the 10 October (Fig. S1), showing the highest concentrations at all sites under NW winds (Fig. S2).

– The sulphate PMF factor profile (Fig. 4g) was defined by $SO_4^{2-}$ and $NH_4^+$ (39 and 73 % of the variation, respectively). OC is also present in significant concentration (around 10 %), suggesting the contribution of secondary organic aerosols to this factor. As a consequence of its regional origin and secondary nature, it shows homogeneous concentration values at the four sites (3.3–4.2 µg m$^{-3}$, 11–17 %; see Table 2).

– The nitrate PMF factor profile (Fig. 4h) was mainly traced by $NO_3^-$ (97 % of the variation), but $NH_4^+$, OC and $Cl^-$ also contributed in a minor proportion (10, 11 and 6 %, respectively). It also shows homogeneous concentration values at the three city sites (around 5.4 µg m$^{-3}$), whereas at TC concentrations were 33 % lower (3.6 µg m$^{-3}$, see Table 2). This revealed a dominant local urban origin of this factor, as nitrate was diluted while being transported to the suburban area.

## 4 Discussion

### 4.1 Variability of aerosol sources across sites and ground-tower ratio

The distance to the emission source strongly influences the concentration levels of certain PMF factors detected at the sampling sites. This is the case of the exhaust and wear and road dust factors, presenting a decreasing concentration gradient with the distance to the traffic hot spots, as the highest concentrations were found at the RS, followed by UB, TM and TC. Regarding the marine factor, the distance to the sea influenced the average concentrations, being highest at TM, followed by RS, UB and TC.





ACPD
15, 33331–33378, 2015



In the case of the industrial factor, whose main source is located SW of the city, the UB was the first site impacted by this plume as it showed the highest concentrations, followed by RS, TC and TM. On the other hand, fairly homogeneous concentrations were recorded at the sites for mineral and heavy oil factors, evidencing that its sources affect the whole urban area. Regarding sulphate, similar concentrations were recorded at the sites, although the higher concentrations displayed at the UB site remain unexplained at this stage. Concerning the nitrate factor, concentrations were found to decrease with the distance to traffic sources from RS to TC. However, at the TM site higher concentrations than at the UB site were recorded due to the elevation of the urban tower site above the ground favouring the formation of particulate nitrate due to colder temperature. Curci et al. (2015) also showed that an important player in determining the upper planetary boundary layer (PBL) aerosol is particulate nitrate, which may reach higher values in the upper PBL (up to 30 %) than in the lower PBL. Overall, the trends are in line with a recent study in a Chinese Tower (Han et al., 2015), suggesting that the impact of primary sources from the ground decreased with the increase of height, while the impact of secondary sources mainly influenced by regional sources becomes more prominent.

To further study the vertical variability in the factors concentrations, the ratios between the average concentrations at the "ground" sites (RS, UB) and "tower" sites (TM, TC) were calculated for each factor, and the result are presented in Fig. 5. Three sources were found to be different between ground and tower levels: exhaust and wear, road dust and industry. The highest differences were found for the exhaust and wear and road dust factors, where the concentrations at the ground sites were 2.8 and 1.8 times those at the towers, respectively. The industrial factor concentration at the ground sites were on average 1.6 times higher than at the towers, pointing towards the greater impact of the SW industrial plume on ground levels; although a contribution of the small industrial facilities spread within the city should not be discarded. Secondary inorganic sulphate and nitrate factors concentrations were slightly higher at the ground than at the tower sites. On the other hand, the remaining factors (mineral factor, aged marine





ACPD
15, 33331–33378, 2015



and heavy oil) showed similar contributions at ground and tower sites. A vertical distribution for various chemical species was also previously reported in a number of other studies. For example, Han et al. (2015) recently showed similar percentage levels at the four different heights for Al and Si. However, for the Ca and EC fractions, higher values were observed at lower sampling sites. The percentages of nitrate, sulphate and OC, and the OC/EC ratios were higher at the higher sites. Source apportionment for ambient $PM_{10}$ showed that the percentage contributions of secondary sources obviously increased with height, while the contribution of cement dust decreased with height. Ho et al. (2015) also reported that vertical variations were observed for mineral and road dust (Si, Ti and Fe) in the $PM_{2.5}$ region. Similarly, Wu et al. (2014) reported traffic related aerosol (in particular resuspended road dust – traced with Si) and industrial ground activities vertically stratified. In summary – consistent with this SAPUSS study – exhaust traffic, non-exhaust traffic and industrial aerosol sources were the ones mostly affecting the aerosol vertical gradients.

### 4.2 Aerosol sources variability relative to air mass category

The variability in $PM_{10}$ concentrations and air mass scenario during SAPUSS (according to the classification presented by Dall'Osto et al., 2013a) shown in Fig. 1 was already briefly discussed in Sect. 3.1. Figure 6 shows the average concentrations at each site under the five air mass scenarios identified during SAPUSS: Atlantic (ATL), Regional (REG), North African West (NAF_W), North African East (NAF_E) and European (EUR). REG scenarios were related to the recirculation of air masses over the study area, thus favouring the accumulation of both primary (vehicle exhaust and wear, industrial) and secondary pollutants (sulphate, nitrate). Overall, concentrations were 32 % higher under these REG air masses due to low pollutants dispersion (Fig. 6). Air masses with an African origin (NAF_W and NAF_E) were influenced mainly by the mineral factor. The NAF_E air mass also crossed the WMB, blowing easterly winds inland and also causing an increase in aged marine aerosols concentration. Under North African air masses (NAF_W and NAF_E), average concentration levels nearly





ACPD
15, 33331–33378, 2015



doubled with respect to the average levels for non-African days (9.2 vs. 4.9 $\mu g\,m^{-3}$, Figs. 5 and 6e and f). The cruise and commercial port of the city is located south of the city (Fig. S2), and thus under NAF_W air masses and S-SW winds the highest heavy oil concentrations were recorded at all sites, pointing towards direct port emissions as the main contributor to this factor. Road dust also showed the highest concentrations during NAF_E scenarios due to the increase of its loading and subsequent resuspension. During the study period EUR air masses were related to a rainfall event, thus wet deposition caused a radical decrease in road dust concentrations under this scenario. A decrease in concentrations of 90 % on average, due to wet deposition and less resuspension, was recorded under EUR air masses, as they were associated with rain during the study period (0.3 vs. 2.7 $\mu g\,m^{-3}$, see Fig. 6c and d). On the other hand the aged marine factor concentrations were found to increase, due to the trajectory followed by this air mass over the Mediterranean Sea. ATL air masses were generally related to low concentrations for the different factors (due to pollutants dilution) except for the industrial factor, which might be explained similarly by the accompanying westerly winds under this scenario.

As discussed in Dall'Osto et al. (2013a), a number of possible REG stagnant different scenarios were classified during SAPUSS. As a case study, we consider two different ones: REG_1 (4 days between 29 September and 2 October) and REG_2 (4 days between 14–17 October). Figure S3 shows the meteorological diurnal profiles of the two scenarios. Whilst REG_1 shows warmer temperatures and a daily sea breeze circulation, REG_2 is characterised by colder temperatures, more stagnant air and an absence of a sea breeze circulation. Overall, high $PM_{10}$ concentrations were recorded under REG air mass due to the accumulation of pollutants. REG_1 presented 19–31 $\mu g\,m^{-3}$ $PM_{10}$ average mass concentrations across the four sites, whereas REG_2 showed even higher loadings (30–41 $\mu g\,m^{-3}$). The REG_1 episode allowed the transport of heavy oil towards the city with the development of the sea breeze, whereas in the REG_2 episode the poor development of the sea breeze minimized the transport of the shipping emissions towards the city (Fig. S3). It is interesting to note that





ACPD
15, 33331–33378, 2015



during the REG_2 recirculation episode (14–17 October), the nitrate PMF factor concentrations were doubled (10.7 vs. 4.9 $\mu g\,m^{-3}$ overall SAPUSS average) at the four monitoring sites, reaching occasionally higher levels at the tower sites (TM, TC) than at ground levels (RS, UB). By contrast, the sulphate PMF factor did not show a larger variation among different REG scenarios. The PMF nitrate/PMF sulphate ratio was found to be 1.2 and 2.3 for REG_1 and REG_2, respectively. As previously observed in a vertical aerosol study in London (Harrison et al., 2012) the cooler temperatures and higher relative humidity on the tower level during the REG_2 scenario can shift the gas/aerosol nitrate equilibrium towards the aerosol phase. In other words, during SAPUSS some aspects of nitrate behaviour were broadly similar to those of sulphate, but other aspects proved very different. During SAPUSS, Aerosol Time-Of-Flight Mass Spectrometer studies (Dall'Osto et al., 2013a) reported two types of nitrate aerosols. Briefly, the first appeared to be associated with local formation processes and occurred at times outside of the long-range transport episode. The second type of nitrate was regionally transported and internally mixed with sulphate, ammonium and both elemental and organic carbon (Dall'Osto et al., 2009). On this regards, it is worth to remember that the nitrate radical ($NO_3$) is amongst the most important oxidants in the nocturnal boundary layer (NBL) (Benton et al., 2010). Little is known about products between the formation of $NO_3$, its reactions with volatile organic compounds (VOCs) and the formation of organic nitrate (Wayne et al., 1991; Brown et al., 2009). The PMF method applied in this aerosol filter based $PM_{10}$ concentrations shows OC being an important component (11 %) for the PMF nitrate factor, although 19 % of the OC component was not described by the PMF and found in the PMF residuals. It is likely that the high concentrations of nitrate found in regional air masses during SAPUSS are a complex mixture of different types of aerosol nitrate, not been distinguished during this PMF analysis and likely due to the poor time resolution (12 h) of the off-line aerosol filter techniques (Dall'Osto et al., 2013a).





ACPD
15, 33331–33378, 2015



### 4.3 Additional aerosol source estimations

The PMF model was applied during this SAPUSS study and the results were presented in Sect. 3.2. However, this statistical tool is usually unable to differentiate between natural and anthropogenic sources contributing to the same factor (Viana et al., 2005). In order to elucidate the contributions to ambient $PM_{10}$ concentrations, a combination of additional aerosol source estimation techniques were applied to further elucidate two main natural sources (mineral dust and sea salt sources) contributing to the $PM_{10}$ mass during SAPUSS in Barcelona.

#### 4.3.1 Mineral dust sources

Mineral sources in a Mediterranean urban environment are diverse. Broadly, three main components of mineral dust have been reported in the literature: (1) urban-regional background dust, (2) local road dust and (3) Saharan dust. Querol et al. (2001) reported a urban/regional background mineral dust factor enriched in Al and Ca, which presented higher concentrations in summer than in winter. A background source rich in Ca, Si, Al and Ti was also attributed to regional anthropogenic and natural resuspension such as urban dust from construction/demolition works, unpaved areas and parks, among other sources (Amato et al., 2009). Road dust is associated with resuspended road dust by passing vehicles and wind, and is traced by Fe, Ca, Al, Si, Ti, Cu, Sb, Sn, Ba, Zn, OC and EC (Schauer et al., 2006). The use of constraints for the source apportionment PMF model by using pulling equations enabled to quantify the road dust fraction of the mineral dust. This PMF factor was characterised by a clear decreasing concentrations gradient with the distance to traffic sources and it contributed with 1.6 to 3.8 $\mu g\,m^{-3}$.

Saharan dust outbreaks transporting dust (made of quartz, clays, calcium carbonate and iron oxide and traced by Al, Si, Ti among others) regularly impact the study area (Querol et al., 2001). Efforts have focused on quantifying this contribution to the average mineral loading, both for air quality purposes (Querol et al., 2009; Pey





ACPD
15, 33331–33378, 2015



et al., 2013) and its impact on population's health (Pérez et al., 2008). However, the PMF factor analysis could not efficiently separate Saharan dust, background mineral and road dust. Hence, the methodology proposed by Escudero et al. (2007) for estimating the Saharan dust daily contribution for different mass fractions was applied. Briefly, it consists in subtracting from the average concentrations registered at the city (Barcelona) those ones simultaneously measured at the nearest regional background site (Montseny, 720 m a.s.l., 50 km NE of Barcelona). However, during SAPUSS the estimated Saharan dust loadings calculated with this method often exceeded the real $PM_{10}$ concentrations registered at the SAPUSS sites. This is likely due to the fact that Saharan dust outbreaks are different at the sea level Barcelona city and its higher altitude regional background surrounding area (Escudero et al., 2007). Therefore, a different methodology was applied for subtracting the Saharan dust load from the mineral factor. We calculated the in situ baseline of mineral dust levels at each site during the Saharan outbreaks, taking into account the concentrations registered before and after the Saharan dust episodes, and extracted these from the mineral dust load for each sample at each site. The resulting concentration excedence of mineral dust was interpreted as the Saharan dust contribution. Overall, it was found that the average contribution of Saharan dust for the whole study period at the four sites was 2.1 $\mu g\,m^{-3}$ (28 % of the $PM_{10}$ mineral load). Upon subtraction of the estimated Saharan dust contribution at each site, the remaining mineral loading corresponds to background mineral dust of urban or regional origin (2.7 to 2.9 $\mu g\,m^{-3}$). This narrow concentration range at the four sites (Fig. 7) – independently of the height and urban location – points towards a regional origin of this background mineral matter.

In summary, during SAPUSS the three mineral dust sources (Figs. 7–9) could be summarised as follow:

1. background dust: it presented a homogeneous distribution among the sampling sites and was thus attributed to background mineral dust with a possible urban or regional origin. A regional origin is thought to be more probable due to the uniform distribution of this dust type at both horizontal and vertical levels for the whole





ACPD
15, 33331–33378, 2015



study area. Average concentrations during the SAPUSS study ranged from 2.7 to 2.9 $\mu g\,m^{-3}$, resulting in the mineral source with the highest contribution (37 % of the mineral dust in $PM_{10}$ in the study period).

2. Road dust: the concentrations decreased from RS to TC, contributing 3.8–1.6 $\mu g\,m^{-3}$ on average (35 % of the mineral dust in $PM_{10}$ during the study period).

3. Saharan dust: African air mass incursions occurred on 20 % of the days during the study period. Under this scenario, the excess dust from the PMF mineral factor was extracted and attributed to Saharan dust, thus obtaining an average Saharan dust contribution of 2.1 $\mu g\,m^{-3}$ (28 % of the mineral dust in $PM_{10}$ in the study period).

#### 4.3.2 Sea salt aerosols

Sea spray aerosol is an important component of the aerosol population in the marine environment, and given that 70 % of the Earth's surface is covered by oceans, it contributes significantly to the global aerosol budget (Vignati et al., 2010). Due to the high impact of anthropogenic activities on the WMB and the frequent recirculation of regional polluted air masses on the region, an interaction between natural and anthropogenic sources is expected. Indeed, 22 % of the variability of $SO_4^{2-}$ was attributed to the aged marine PMF factor (Fig. 4, Table S2), suggesting that this factor is internally mixed with anthropogenic pollutants. The corresponding ss Na associated with nss $SO_4^{2-}$ was calculated and subtracted from the stoichiometrically calculated sea salt, in order to differentiate between the calculated sea salt and the anthropogenic marine sulphate contributions to this PMF factor. The PMF aged marine factor (2.6–5.2 $\mu g\,m^{-3}$) could be broken down into calculated fresh sea salt (1.2–2.1 $\mu g\,m^{-3}$, 40–47 %) and anthropogenic marine sulphate of regional origin (1.4–3.1 $\mu g\,m^{-3}$, 53–60 %). These results evidence that both the calculated sea salt and the anthropogenic marine sulphate aerosols contributed in a similar proportion to the aged marine factor (Figs. 8 and 9). The marine sulphate of anthropogenic origin derived from the aged marine fac-





ACPD
15, 33331–33378, 2015



tor shows a different origin to the PMF sulphate factor. As can be seen in Fig. S2 the highest concentrations of anthropogenic marine sulphate were recorded under eastern winds at all sites, whereas for the PMF sulphate factor no dominant wind direction was found. Namely, the highest sulphate factor concentrations were recorded under REG air masses while the anthropogenic marine sulphate shows relatively low concentrations. Conversely, under NAF_E air masses the marine sulphate of regional origin shows the highest concentrations, contrarily to the secondary sulphate factor (Fig. S1).

## 5 Conclusions

With the aim of assessing and evaluating the vertical and horizontal spatial variability of $PM_{10}$ concentrations in a Southern European urban environment, 221 $PM_{10}$ samples (12 h resolution) were simultaneously collected at four monitoring sites strategically located within the city of Barcelona during one month (SAPUSS campaign, 20 September to 20 October 2010). A decreasing $PM_{10}$ concentration gradient from road traffic hot spots to the background areas was recorded. Overall, both the proximity to traffic sources and the different types of air mass scenarios lead to a wide variability in concentrations and chemical composition of $PM_{10}$ across the vertical and horizontal scale in Barcelona during SAPUSS. When a PMF factor analysis was run on the 221 filters sampled collected, the optimal chosen solution contained eight factors: (1) vehicle exhaust and wear, (2) road dust, (3) mineral, (4) aged marine, (5) heavy oil, (6) industrial, (7) sulphate and (8) nitrate. Overall, primary traffic emissions (exhaust and wear and road dust) accounted for 18–39 % of $PM_{10}$ mass, primary inorganic aerosols (mineral dust and aged marine) 27–39 %, industry (heavy oil and industrial) 5–7 % and secondary aerosols (sulphate and nitrate) 28–36 %. The main factors influencing the different sources concentration at each site were: air mass origin, proximity to the emission source and meteorological parameters, such as wind speed and direction (influencing the sea breeze development for both dispersion and transport of specific pollutants) and temperature (causing the volatilization of nitrate under high temperatures).





ACPD
15, 33331–33378, 2015



Special emphasis was put in trying to further apportion the dust aerosol sources. Overall, three sources of dust were identified in the urban area of Barcelona: road dust (3.8–1.6 $\mu g\,m^{-3}$, average 35 %), Saharan dust (2.1 $\mu g\,m^{-3}$, average 28 %) and mineral dust of regional origin (2.7–2.9 $\mu g\,m^{-3}$, average 38 %). Regarding the aged marine aerosol factor, it was found to be internally mixed with sulphate of regional origin, as the calculated fresh sea salt (1.8 $\mu g\,m^{-3}$, 45 % of the aerosol marine load) was aged by the mixing with anthropogenic marine sulphate of regional origin (2.2 $\mu g\,m^{-3}$, 55 % of the aerosol marine load). As expected, it was found that non vehicle exhausts, vehicle exhausts, and local industries located in the city centre were contributing to the $PM_{10}$ ground concentrations levels. However, surprisingly the $PM_{10}$ concentrations of secondary aerosols were found more homogeneous than expected. On the whole, our results show that although a higher homogeneity than expected was found in the horizontal and vertical variability of pollution levels in the Barcelona urban atmosphere, primary emission factors related to vehicle exhaust emissions and road dust resuspension decrease with the distance to traffic hot spots. Road traffic emissions comprise not only tailpipe exhaust emissions but also non-exhaust emissions derived from the vehicle-induced resuspension of dust deposited on the road, and from the direct emissions from vehicle wear (brakes, tyres, discs etc.). This study confirms that – for the coarse $PM_{10}$ fraction – road traffic is still a major source of ground level $PM_{10}$ aerosol mass. Furthermore, this study shows that local industries-small workplaces are also a source of $PM_{10}$ aerosol mass within urban ground levels.

**The Supplement related to this article is available online at doi:10.5194/acpd-15-33331-2015-supplement.**

*Acknowledgements.* This study was supported by FP7-PEOPLE-2009-IEF, project number 254 773, SAPUSS – Solving Aerosol Problems Using Synergistic Strategies (Marie Curie Actions –Intra European Fellowships. Manuel Dall'Osto). This study was also supported by research projects from the D.G. de Calidad y Evaluación Ambiental (Spanish Ministry of the





ACPD
15, 33331–33378, 2015



Environment) and the Plan Nacional de I+D (Spanish Ministry of Science and Innovation (CGL2010-19 464 (VAMOS) and CSD2007-00 067 (GRACCIE))). Finally, Santiago Castante (Mapfre Tower), Diego Garcia Talavera (Collserola tower) and Alfons Puertas (Secció de Meteorologia, Fabra Observatory) are also acknowledged.

## References

Agrawal, H., Malloy, Q. G. J., Welch, W. A., Miller, J. W., and Cocker, D. R.: In-use gaseous and particulate matter emissions from a modern ocean going container vessel, Atmos. Environ., 42, 5504–5510, 2008.

Amato, F., Pandolfi, M., Escrig, A., Querol, X., Alastuey, A., Pey, J., Perez, N., and Hopke, P. K.: Quantifying road dust resuspension in urban environment by Multilinear Engine: a comparison with PMF2, Atmos. Environ., 43, 2770–2780, 2009.

Amato, F., Alastuey, A., Karanasiou, A., Lucarelli, F., Nava, S., Calzolai, G., Severi, M., Becagli, S., Gianelle, V. L., Colombi, C., Alves, C., Custódio, D., Nunes, T., Cerqueira, M., Pio, C., Eleftheriadis, K., Diapouli, E., Reche, C., Minguillón, M. C., Manousakas, M., Maggos, T., Vratolis, S., Harrison, R. M., and Querol, X.: AIRUSE-LIFE+: a harmonized PM speciation and source apportionment in 5 Southern European cities, Atmos. Chem. Phys. Discuss., 15, 23989–24039, doi:10.5194/acpd-15-23989-2015, 2015.

Beddows, D. C. S., Harrison, R. M., Green, D. C., and Fuller, G. W.: Receptor modelling of both particle composition and size distribution from a background site in London, UK, Atmos. Chem. Phys., 15, 10107–10125, doi:10.5194/acp-15-10107-2015, 2015.

Benton, A. K., Langridge, J. M., Ball, S. M., Bloss, W. J., Dall'Osto, M., Nemitz, E., Harrison, R. M., and Jones, R. L.: Night-time chemistry above London: measurements of $NO_3$ and $N_2O_5$ from the BT Tower, Atmos. Chem. Phys., 10, 9781–9795, doi:10.5194/acp-10-9781-2010, 2010.

Birch, M. E. and Cary, R. A.: Elemental carbon-based method for monitoring occupational exposures to particulate diesel exhaust, Aerosol Sci. Tech., 25, 221–241, 1996.

Brown, S. S., deGouw, J. A., Warneke, C., Ryerson, T. B., Dubé, W. P., Atlas, E., Weber, R. J., Peltier, R. E., Neuman, J. A., Roberts, J. M., Swanson, A., Flocke, F., McKeen, S. A., Brioude, J., Sommariva, R., Trainer, M., Fehsenfeld, F. C., and Ravishankara, A. R.: Nocturnal isoprene oxidation over the Northeast United States in summer and its impact on





ACPD
15, 33331–33378, 2015



reactive nitrogen partitioning and secondary organic aerosol, Atmos. Chem. Phys., 9, 3027–3042, doi:10.5194/acp-9-3027-2009, 2009.

Carslaw, D. C. and Ropkins, K.: Openair – an R package for air quality and data analysis, Environ. Modell. Softw., 27–28, 52–61, 2012.

Cavalli, F., Viana, M., Yttri, K. E., Genberg, J., and Putaud, J.-P.: Toward a standardised thermal-optical protocol for measuring atmospheric organic and elemental carbon: the EUSAAR protocol, Atmos. Meas. Tech., 3, 79–89, doi:10.5194/amt-3-79-2010, 2010.

Chan, C. Y., Xu, X. D., Li, Y. S., Wong, K. H., Ding, G. A., Chan, L. Y., and Cheng, X. H.: Characteristics of vertical profiles and sources of $PM_{2.5}$, $PM_{10}$ and carbonaceous species in Beijing, Atmos. Environ., 39, 5113–5124, doi:10.1016/j.atmosenv.2005.05.009, 2005.

Curci, G., Ferrero, L., Tuccella, P., Barnaba, F., Angelini, F., Bolzacchini, E., Carbone, C., Denier van der Gon, H. A. C., Facchini, M. C., Gobbi, G. P., Kuenen, J. P. P., Landi, T. C., Perrino, C., Perrone, M. G., Sangiorgi, G., and Stocchi, P.: How much is particulate matter near the ground influenced by upper-level processes within and above the PBL? A summertime case study in Milan (Italy) evidences the distinctive role of nitrate, Atmos. Chem. Phys., 15, 2629–2649, doi:10.5194/acp-15-2629-2015, 2015.

Dall'Osto, M., Harrison, R. M., Coe, H., Williams, P. I., and Allan, J. D.: Real time chemical characterization of local and regional nitrate aerosols, Atmos. Chem. Phys., 9, 3709–3720, doi:10.5194/acp-9-3709-2009, 2009.

Dall'Osto, M., Querol, X., Alastuey, A., Minguillon, M. C., Alier, M., Amato, F., Brines, M., Cusack, M., Grimalt, J. O., Karanasiou, A., Moreno, T., Pandolfi, M., Pey, J., Reche, C., Ripoll, A., Tauler, R., Van Drooge, B. L., Viana, M., Harrison, R. M., Gietl, J., Beddows, D., Bloss, W., O'Dowd, C., Ceburnis, D., Martucci, G., Ng, N. L., Worsnop, D., Wenger, J., Mc Gillicuddy, E., Sodeau, J., Healy, R., Lucarelli, F., Nava, S., Jimenez, J. L., Gomez Moreno, F., Artinano, B., Prévôt, A. S. H., Pfaffenberger, L., Frey, S., Wilsenack, F., Casabona, D., Jiménez-Guerrero, P., Gross, D., and Cots, N.: Presenting SAPUSS: Solving Aerosol Problem by Using Synergistic Strategies in Barcelona, Spain, Atmos. Chem. Phys., 13, 8991–9019, doi:10.5194/acp-13-8991-2013, 2013a.

Dall'Osto, M., Querol, X., Amato, F., Karanasiou, A., Lucarelli, F., Nava, S., Calzolai, G., and Chiari, M.: Hourly elemental concentrations in $PM_{2.5}$ aerosols sampled simultaneously at urban background and road site during SAPUSS – diurnal variations and PMF receptor modelling, Atmos. Chem. Phys., 13, 4375–4392, doi:10.5194/acp-13-4375-2013, 2013b.





ACPD
15, 33331–33378, 2015



Deng, X. J., Li, F., Li, Y. H., Li, J. Y., Huang, H. Z., and Liu, X. T.: Vertical distribution characteristics of PM in the surface layer of Guangzhou, Particuology, 20, 3–9, 2015.

Dirección General de Tráfico (DGT), available at: http://www.dgt.es/es/seguridad-vial/estadisticas-e-indicadores/parque-vehiculos/, last access: November 2015.

Eeftens, M., Tsai, M.-Y., Ampe, C., Anwander, B., Beelen, R., Bellander, T., Cesaroni, G., Cirach, M., Cyrys, J., de Hoogh, K., De Nazelle, A., de Vocht, F., Declercq, C., Dėdelė, A., Eriksen, K., Galassi, C., Gražulevičienė, R., Grivas, G., Heinrich, J., Hoffmann, B., Iakovides, M., Ineichen, A., Katsouyanni, K., Korek, M., Krämer, U., Kuhlbusch, T., Lanki, T., Madsen, C., Meliefste, K., Mölter, A., Mosler, G., Nieuwenhuijsen, M., Oldenwening, M., Pennanen, A., Probst-Hensch, N., Quass, U., Raaschou-Nielsen, O., Ranzi, A., Stephanou, E., Sugiri, D., Udvardy, O., Vaskövi, É., Weinmayr, G., Brunekreef, B., and Hoek, G.: Spatial variation of $PM_{2.5}$, $PM_{10}$, $PM_{2.5}$ absorbance and PM coarse concentrations between and within 20 European study areas and the relationship with $NO_2$ – results of the ESCAPE project, Atmos. Environ., 62, 303–317, 2012.

Efron, B. and Tibshirani, R.: Bootstrap methods for standard errors, confidence intervals, and other measures of statistical accuracy, Stat. Sci., 1, 54–75, 1986.

Escrig Vidal, A., Monfort, E., Celades, I., Querol, X., Amato, F., Minguillón, M. C., and Hopke, P. K.: Application of optimally scaled target factor analysis for assessing source contribution of ambient $PM_{10}$, JAPCA J. Air Waste Ma., 59, 1296–1307, 2009.

Escudero, M., Querol, X., Pey, J., Alastuey, A., Pérez, N., Ferreira, F., Alonso, S., Rodríguez, S., and Cuevas, E.: A methodology for the quantification of the net African dust load in air quality monitoring networks, Atmos. Environ., 41, 5516–5524, 2007.

Ferrero, L., Perrone, M. G., Petraccone, S., Sangiorgi, G., Ferrini, B. S., Lo Porto, C., Lazzati, Z., Cocchi, D., Bruno, F., Greco, F., Riccio, A., and Bolzacchini, E.: Vertically-resolved particle size distribution within and above the mixing layer over the Milan metropolitan area, Atmos. Chem. Phys., 10, 3915–3932, doi:10.5194/acp-10-3915-2010, 2010.

Ferrero, L., Castelli, M., Ferrini, B. S., Moscatelli, M., Perrone, M. G., Sangiorgi, G., D'Angelo, L., Rovelli, G., Moroni, B., Scardazza, F., Močnik, G., Bolzacchini, E., Petitta, M., and Cappelletti, D.: Impact of black carbon aerosol over Italian basin valleys: high-resolution measurements along vertical profiles, radiative forcing and heating rate, Atmos. Chem. Phys., 14, 9641–9664, doi:10.5194/acp-14-9641-2014, 2014.

Han, S., Zhang, Y., Wu, J., Zhang, X., Tian, Y., Wang, Y., Ding, J., Yan, W., Bi, X., Shi, G., Cai, Z., Yao, Q., Huang, H., and Feng, Y.: Evaluation of regional background particulate





ACPD
15, 33331–33378, 2015



matter concentration based on vertical distribution characteristics, Atmos. Chem. Phys., 15, 11165–11177, doi:10.5194/acp-15-11165-2015, 2015.
Harrison, R. M., Dall'Osto, M., Beddows, D. C. S., Thorpe, A. J., Bloss, W. J., Allan, J. D., Coe, H., Dorsey, J. R., Gallagher, M., Martin, C., Whitehead, J., Williams, P. I., Jones, R. L., Langridge, J. M., Benton, A. K., Ball, S. M., Langford, B., Hewitt, C. N., Davison, B., Martin, D., Petersson, K. F., Henshaw, S. J., White, I. R., Shallcross, D. E., Barlow, J. F., Dunbar, T., Davies, F., Nemitz, E., Phillips, G. J., Helfter, C., Di Marco, C. F., and Smith, S.: Atmospheric chemistry and physics in the atmosphere of a developed megacity (London): an overview of the REPARTEE experiment and its conclusions, Atmos. Chem. Phys., 12, 3065–3114, doi:10.5194/acp-12-3065-2012, 2012.
Ho, C.-C., Chan, C.-C., Cho, C.-W., Lin, H.-I., Lee, J.-H., and Wu, C.-F.: Land use regression modelling with vertical distribution measurements for fine particulate matter and elements in an urban area, Atmos. Environ., 104, 256–263, 2015.
Karanasiou, A., Diapouli, E., Cavalli, F., Eleftheriadis, K., Viana, M., Alastuey, A., Querol, X., and Reche, C.: On the quantification of atmospheric carbonate carbon by thermal/optical analysis protocols, Atmos. Meas. Tech., 4, 2409–2419, doi:10.5194/amt-4-2409-2011, 2011.
Karanasiou, A., Querol, X., Alastuey, A., Perez, N., Pey, J., Perrino, C., Berti, G., Gandini, M.,Poluzzi, V., Ferrari, S., de la Rosa, J., Diaz, J., Pascal, M., Samoli, E., Kelesis, A., Sunyer, J., Alessandrini, E., Stafoggia, M., Forastiere, F., and the Med Particles Study Group: Particulate matter and gaseous pollutants in the Mediterranean Basin: results from the MedParticles 5 project, Sci. Total Environ., 488–489, 297–315, 2014.
Kassomenos, P. A., Vardoulakis, S., Chaloulakou, A., Paschalidou, A. K., Grivas, G., Borge, R., and Lumbreras, J.: Study of $PM_{10}$ and $PM_{2.5}$ levels in three European cities: analysis of intra and inter urban variations, Atmos. Environ., 87, 153–163, 2014.
Kelly, F. J. and Fussell, J. C.: Size, source and chemical composition as determinants of toxicity attributable to ambient particulate matter, Atmos. Environ., 60, 504–526, 2012.
Kim, E. and Hopke, P. K.: Source characterization of ambient fine particles at multiple sites in the Seattle area, Atmos. Environ., 42, 6047–6056, 2008.
Lim, S. S., Vos, T., Flaxman, A. D., Danaei, G., Shibuya, K., Adair-Rohani, H., Amann, M., Anderson, H. R., Andrews, K. G., Aryee, M., Atkinson, C. Bacchus, L. J., Bahalim, A. N., Balakrishnan, K., Balmes, J., Barker-Collo, S., Baxter, A., Bell, M. L., Blore, J. D., Blyth, F., Bonner, C., Borges, G., Bourne, R., Boussinesq, M., Brauer, M., Brooks, P., Bruce, N. G., Brunekreef, B., Bryan-Hancock, C., Bucello, C., Buchbinder, R., Bull, F., Burnett, R. T.,





ACPD
15, 33331–33378, 2015



Byers, T. E., Calabria, B., Carapetis, J., Carnahan, E., Chafe, Z., Charlson, F., Chen, H., Chen, J. S., Cheng, A. T., Child, J. C., Cohen, A., Colson, K. E., Cowie, B. C., Darby, S., Darling, S., Davis, A., Degenhardt, L., Dentener, F., Jarlais, D. C. Des, Devries, K., Dherani, M., Ding, E. L., Dorsey, E. R., Giovannucci, E., Gmel, G., Graham, K., Grainger, R., Grant, B., Gunnell, D., Gutierrez, H. R., Hall, W., Room, R., Rosenfeld, L. C., Roy, A., Rushton, L., Salomon, J. A., Sampson, U., Sanchez-Riera, L., Sanman, E., Stapelberg, N. J. C., Steenland, K., Stöckl, H., Stovner, L. J., Straif, K., Straney, L., Thurston, G. D., Tran, J. H., Whiteford, H., Wiersma, S. T., Wilkinson, J. D., Williams, H. C., Williams, W., Wilson, N., Woolf, A. D., Yip, P., Zielinski, J. M., Lopez, A. D., Murray, C. J. L., and Ezzati, M.: A comparative risk assessment of burden of disease and injury attributable to 67 risk factors and risk factor clusters in 21 regions, 1990–2010: a systematic analysis for the Global Burden of Disease Study 2010, J. Lancet, 380, 2224–2260, doi:10.1016/S0140-6736(12)61766-8, 2012.

Mason, B.: Principles of Geochemistry, 3rd edn., Wiley, New York, 1966.

Mészáros, E.: Fundamentals of Atmospheric Aerosol Chemistry, Akadémiai Kiado, Budapest, 1999.

Minguillón, M. C., Perron, N., Querol, X., Szidat, S., Fahrni, S. M., Alastuey, A., Jimenez, J. L., Mohr, C., Ortega, A. M., Day, D. A., Lanz, V. A., Wacker, L., Reche, C., Cusack, M., Amato, F., Kiss, G., Hoffer, A., Decesari, S., Moretti, F., Hillamo, R., Teinilä, K., Seco, R., Peñuelas, J., Metzger, A., Schallhart, S., Müller, M., Hansel, A., Burkhart, J. F., Baltensperger, U., and Prévôt, A. S. H.: Fossil versus contemporary sources of fine elemental and organic carbonaceous particulate matter during the DAURE campaign in Northeast Spain, Atmos. Chem. Phys., 11, 12067–12084, doi:10.5194/acp-11-12067-2011, 2011.

Minguillón, M. C., Cirach, M., Hoek, G., Brunekreef, B., Tsai, M., de Hoogh, K., Jedynska, A., Kooter, I. M., Nieuwenhuijsen, M., and Querol, X.: Spatial variability of trace elements and sources for improved exposure assessment in Barcelona, Atmos. Environ., 89, 268–281, doi:10.1016/j.atmosenv.2014.02.047, 2014.

Moeinaddini, M., Esmaili Sari, A., Riyahi bakhtiari, A., Chan, A. Y. C., Taghavi, S. M., Hawker, D., and Connell, D.: Source apportionment of PAHs and n-alkanes in respirable particles in Tehran, Iran by wind sector and vertical profile, Environ. Sci. Pollut. R., 21, 7757–7772, doi:10.1007/s11356-014-2694-1, 2014.





ACPD
15, 33331–33378, 2015



Moreno, T., Querol, X., Castillo, S., Alastuey, A., Cuevas, E., Herrmann, L., Mounkaila, M., Elvira, J., and Gibbons, W.: Geochemical variations in aeolian mineral particles from the Sahara–Sahel Dust Corridor, Chemosphere, 65, 2, 261–270, 2006.

Moreno, T., Querol, X., Alastuey, A., Reche, C., Cusack, M., Amato, F., Pandolfi, M., Pey, J., Richard, A., Prévôt, A. S. H., Furger, M., and Gibbons, W.: Variations in time and space of trace metal aerosol concentrations in urban areas and their surroundings, Atmos. Chem. Phys., 11, 9415–9430, doi:10.5194/acp-11-9415-2011, 2011.

Norman, M. and Johansson, C.: Studies of some measures to reduce road dust emissions from paved roads in Scandinavia, Atmos. Environ., 40, 6154–6164, 2006.

Ntziachristos, L., Ning, Z., Geller, M. D., and Sioutas, C.: Particle concentration and characteristics near a major freeway with heavy-duty diesel traffic, Environ. Sci. Technol., 41, 2223–2230, 2007.

Öztürk, F., Bahreini, R., Wagner, N. L., Dubé, W. P., Young, C. J., Brown, S. S., Brock, C. A., Ulbrich, I. M., Jimenez, J. L., Cooper, O. R., and Middlebrook, A. M.: Vertically resolved chemical characteristics and sources of submicron aerosols measured on a Tall Tower in a suburban area near Denver, Colorado in winter, J. Geophys. Res.-Atmos., 118, 13591–13605, doi:10.1002/2013JD019923, 2013.

Paatero, P.: The multilinear engine – a table-driven, least squares program for solving multilinear problems, including the n-way parallel factor analysis model, J. Comput. Graph. Stat., 8, 854–888, 1999.

Paatero, P.: End User's Guide to Multilinear Engine Applications, ME2 Software, 2007.

Paatero, P. and Hopke, P. K.: Discarding or downweighting high-noise variables in factor analytic models, Anal. Chim. Acta, 25, 277–289, 2003.

Paatero, P. and Hopke, P. K.: Rotational tools for factor analytic models implemented by using 10 the multilinear engine, J. Chemometr., 23, 91–100, 2008.

Paatero, P. and Hopke, P. K.: Rotational tools for factor analytic models, J. Chemometr., 23, 91–100, 2009.

Paatero, P. and Tapper, U.: Positive matrix factorization: a non-negative factor model with optimal utilization of error estimates of data values, Environmetrics, 5, 111–126, 1994.

Pandolfi, M., Martucci, G., Querol, X., Alastuey, A., Wilsenack, F., Frey, S., O'Dowd, C. D., and Dall'Osto, M.: Continuous atmospheric boundary layer observations in the coastal urban area of Barcelona during SAPUSS, Atmos. Chem. Phys., 13, 4983–4996, doi:10.5194/acp-13-4983-2013, 2013.





ACPD
15, 33331–33378, 2015



Pandolfi, M., Querol, X., Alastuey, A., Jimenez, J. L., Jorba, O., Day, D., Ortega, A., Cubison, M. J., Comerón, A., Sicard, M., Mohr, C., Prévôt, A. S. H., Minguillón, M. C., Pey, J., Baldasano, J. M., Burkhart, J. F., Seco, R., Peñuelas, J., van Drooge, B. L., Artiñano, B., Di Marco, C., Nemitz, E., Schallhart, S., Metzger, A., Hansel, A., Lorente, J., Ng, S., Jayne, J., and Szidat, S.: Effects of sources and meteorology on particulate matter in the Western Mediterranean Basin: an overview of the DAURE campaign, J. Geophys. Res.-Atmos., 119, 4978–5010, doi:10.1002/2013JD021079, 2014.

Pérez, L., Tobias, A., Querol, X., Künzli, N, Pey, J., Alastuey, A., Viana, M., Valero, N., González-Cabré, M., and Sunyer, J.: Coarse particles from Saharan dust and daily mortality, J. Epidemiol., 19, 800–807, 2008.

Pérez, N., Pey, J., Cusack, M., Reche, C., Querol, X., Alastuey, A., and Viana, M.: Variability of particle number, black carbon, and $PM_{10}$, $PM_{2.5}$, and $PM_1$ levels and speciation: influence of road traffic emissions on urban air quality, Aerosol Sci. Tech., 44, 487–499, 2010.

Pey, J., Querol, X., and Alastuey, A.: Discriminating the regional and urban contributions in the North-Western Mediterranean: PM levels and composition, Atmos. Environ., 44, 1587–1596, 2010.

Pey, J., Querol, X., and Alastuey, A.: $PM_{10}$ and $PM_{2.5}$ sources at an insular location in the western Mediterranean by using source apportionment techniques, Sci. Total Environ., 456–457, 267–277, 2013.

Pope, C. A. and Dockery, D. W.: Health effects of fine particulate air pollution: lines that connect, J. Air Waste Manage., 56, 709–742, doi:10.1080/10473289.2006.10464485, 2006.

Pope, C. A., Ezzati, M., and Dockery, D. W.: Fine-particulate air pollution and life expectancy in the United States, New Engl. J. Med., 360, 376–386, doi:10.1056/NEJMsa0805646, 2009.

Putaud, J.-P., Van Dingenen, R., Alastuey, A., Bauer, H., Birmili, W., Cyrys, J., Flentje, H., Fuzzi, S., Gehrig, R., Hansson, H. C., Harrison, R. M., Herrmann, H., Hitzenberger, R., Hüglin, C., Jones, A. M., Kasper-Giebl, A., Kiss, G., Kousa, A., Kuhlbusch, T. A. J., Löschau, G., Maenhaut, W., Molnár, A., Moreno, T., Pekkanen, J., Perrino, C., Pitz, M., Puxbaum, H., Querol, X., Rodriguez, S., Salma, I., Schwarz, J., Smolik, J., Schneider, J., Spindler, G., ten Brink, H., Tursic, J., Viana, M., Wiedensohler, A., and Raes, F.: A European aerosol phenomenology – 3: physical and chemical characteristics of particulate matter from 60 rural, urban, and kerbside sites across Europe, Atmos. Environ., 44, 1308–1320, 2010.

Puxbaum, H., Caseiro, A., Sánchez-Ochoa, A., Kasper-Giebl, A., Claeys, M., Gelencsér, A., Legrand, M., Preunkert, S., and Pio, C. A.: Levoglucosan levels at background sites in Europe





ACPD
15, 33331–33378, 2015



for assessing the impact of biomass combustion on the European aerosol background, J. Geophys. Res.-Atmos., 112, 1–11, doi:10.1029/2006JD008114, 2007.
Querol, X., Alastuey, A., Rodriguez, S., Plana, F., Ruiz, C. R., Cots, N., Massagué, G., and Puig, O.: $PM_{10}$ and $PM_{2.5}$ source apportionment in the Barcelona Metropolitan area, Catalonia, Spain, Atmos. Environ., 35, 6407–6419, 2001.
Querol, X., Alastuey, A., Pey, J., Cusack, M., Pérez, N., Mihalopoulos, N., Theodosi, C., Gerasopoulos, E., Kubilay, N., and Koçak, M.: Variability in regional background aerosols within the Mediterranean, Atmos. Chem. Phys., 9, 4575–4591, doi:10.5194/acp-9-4575-2009, 2009.
R Development Core Team: R: a language and environment for statistical computing. R Foundation for Statistical Computing, Vienna, Austria, available at: http://www.R-project.org/ (last access: November 2015), 2012.
Reche, C., Viana, M., Amato, F., Alastuey, A., Moreno, T., Hillamo, R., Teinilä, K., Saarnio, K., Seco, R., Peñuelas, J., Mohr, C., Prévôt, A. S. H., Querol, X.: Biomass burning contributions to urban aerosols in a coastal Mediterranean City, Sci. Total Environ., 427–428, 175–190, 2012.
Schauer, J. J., Lough, G.C, Shafer, M. M., Christensen, W. F., Arndt, M. F., DeMinter, J. T., and Park, J.-S.: Characterization of Metals emitted from Motor Vehicles, Research Report 133, Health Effects Institute, Boston, MA, 2006.
Shi, G. L., Tian, Y. Z., Han, S. Q., Zhang, Y. F., Li, X., Feng, Y. C., Wu, J. H., and Zhu, T.: Vertical characteristics of carbonaceous species and their source contributions in a Chinese mega city, Atmos. Environ., 60, 358–365, doi:10.1016/j.atmosenv.2012.06.069, 2012.
Srimuruganandam, B. and Shiva Nagendra, S. M.: Application of positive matrix factorization in characterization of $PM_{10}$ and $PM_{2.5}$ emission sources at urban roadside, Chemosphere, 88, 120–130, doi:10.1016/j.chemosphere.2012.02.083, 2012.
Sternbeck, J., Sjödin, A., and Andréasson, K.: Metal emissions from road traffic and the influence of resuspension results from two tunnel studies, Atmos. Environ., 36, 4735–4744, 2002.
Sun, Y., Song, T., Tang, G., and Wang, Y.: The vertical distribution of PM 2.5 and boundary-layer structure during summer haze in Beijing, Atmos. Environ., 74, 413–421, 2013.
Tao, S., Wang, Y., Wu, S., Liu, S., Dou, H., Liu, Y., Lang, C., Hu, F., and Xing, B.: Vertical distribution of polycyclic aromatic hydrocarbons in atmospheric boundary layer of Beijing in winter, Atmos. Environ., 41, 9594–9602, doi:10.1016/j.atmosenv.2007.08.026, 2007.





ACPD
15, 33331–33378, 2015



Tian, Y. Z., Shi, G. L., Han, S. Q., Zhang, Y. F., Feng, Y. C., Liu, G. R., Gao, L. J., Wu, J. H., and Zhu, T.: Vertical characteristics of levels and potential sources of water-soluble ions in $PM_{10}$ in a Chinese megacity, Sci. Total Environ., 447, 1–9, doi:10.1016/j.scitotenv.2012.12.071, 2013.

Tukey, J. W.: Bias and confidence in not-quite large samples, Ann. Math. Stat., 29, 2, 614, 1958.

Turpin, B. J. and Lim, H.-J.: Species contributions to $PM_{2.5}$ mass concentrations: revisiting common assumptions for estimating organic mass, Aerosol Sci. Tech., 35, 602–610, doi:10.1080/02786820119445, 2001.

Viana, M., Pérez, C., Querol, X., Alastuey, A., Nickovic, S., and Baldasano, J. M.: Spatial and temporal variability of PM levels and composition in complex summer atmospheric scenario in Barcelona (NE Spain), Atmos. Environ., 39, 5343–5361, 2005.

Viana, M., Kuhlbusch, T. A. J., Querol, X., Alastuey, A., Harrison, R. M., Hopke, P. K., Winiwarter, W., Vallius, M., Szidat, S., Prévôt, A. S. H., Hueglin, C., Bloemen, H., Wåhlin, P., Vecchi, R., Miranda, A. I., Kasper-Giebl, A., Maenhaut, W., and Hitzenberger, R.: Source apportionment of particulate matter in Europe: a review of methods and results, J. Aerosol Sci., 39, 827–849, doi:10.1016/j.jaerosci.2008.05.007, 2008.

Viana, M., Hammingh, P., Colette, A., Querol, X., Degraeuwe, B., Vlieger, I. De, and van Aardenne, J.: Impact of maritime transport emissions on coastal air quality in Europe, Atmos. Environ., 90, 96–105, doi:10.1016/j.atmosenv.2014.03.046, 2014.

Vignati, E., Facchini, M. C., Rinaldi, M., Scannell, C., Ceburnis, D.,Sciare, J., Kanakidou, M., Myriokefalitakis, S., Dentener, F., and O'Dowd, C. D.: Global scale emission and distribution of seaspray aerosol: sea-salt and organic enrichment, Atmos. Environ., 44, 670–677, doi:10.1016/j.atmosenv.2009.11.013, 2010.

Waked, A., Favez, O., Alleman, L. Y., Piot, C., Petit, J.-E., Delaunay, T., Verlinden, E., Golly, B., Besombes, J.-L., Jaffrezo, J.-L., and Leoz-Garziandia, E.: Source apportionment of $PM_{10}$ in a north-western Europe regional urban background site (Lens, France) using positive matrix factorization and including primary biogenic emissions, Atmos. Chem. Phys., 14, 3325–3346, doi:10.5194/acp-14-3325-2014, 2014.

Wayne, R. P., Barnes, I., Biggs, P., Burrows, J. P., Canasa-Mas, C. E., Hjorth, J., Le Bras, G., Moorgat, G. K., Perner, D., Poulet, G., Restelli, G., and Sidebottom, H.: The nitrate radical physics, chemistry, and the atmosphere, Atmos. Environ., 25, 1–203, 1991.





ACPD
15, 33331–33378, 2015



Wu, C.-D. and Lung, S.-C. C.: Applying GIS and fine-resolution digital terrain models to assess three-dimensional population distribution under traffic impacts, J. Expo. Sci. Env. Epid., 22, 126–134, 2012.

Wu, C. F., Lin, H. I., Ho, C. C., Yang, T. H., Chen, C. C., and Chan, C. C.: Modelling horizontal and vertical variation in intraurban exposure to $PM_{2.5}$ concentrations and compositions, Environ. Res., 133, 96–102, doi:10.1016/j.envres.2014.04.038, 2014.

Xiao, Z., Wu, J., Han, S., Zhang, Y., Xu, H., Zhang, X., Shi, G., and Feng, Y.: Vertical characteristics and source identification of $PM_{10}$ in Tianjin, J. Environ. Sci., 24, 112–115, doi:10.1016/S1001-0742(11)60734-1, 2012.

Yin, J., Allen, A. G., Harrison, R. M., Jennings, S. G., Wright, E., Fitzpatrick, M., Healy, T., Barry, E., Ceburnis, D., and McCusker, D.: Major component composition of urban $PM_{10}$ and $PM_{2.5}$ in Ireland, Atmos. Res., 78, 149–165, doi:10.1016/j.atmosres.2005.03.006, 2005.

Zhang, Y. F., Xu, H., Tian, Y. Z., Shi, G. L., Zeng, F., Wu, J. H., Zhang, X. Y., Li, X., Zhu, T., and Feng, Y. C.: The study on vertical variability of $PM_{10}$ and the possible sources on a 220 m tower, in Tianjin, China, Atmos. Environ., 45, 6133–6140, doi:10.1016/j.atmosenv.2011.08.040, 2011.





ACPD
15, 33331–33378, 2015



**Table 1.** Mean concentrations of $PM_{10}$ ($\mu g\,m^{-3}$) and their major components during the SAPUSS campaign at the Road Site (RS), Urban Background (UB), Torre Mapfre (TM) and Torre Collserola (TC).

| Species ($\mu g\,m^{-3}$) | Road Site (RS) | Urban Background (UB) | Torre Mapfre (TM) | Torre Collserola (TC) |
|---|---|---|---|---|
| $PM_{10}$ | 30.7 (100 %) | 25.9 (100 %) | 24.8 (100 %) | 21.8 (100 %) |
| Crustal | 5.2 (17 %) | 4.0 (15 %) | 3.6 (14 %) | 3.1 (14 %) |
| Sea salt | 2.6 (9 %) | 2.1 (8 %) | 2.7 (11 %) | 1.5 (7 %) |
| $NO_3^-$ | 2.6 (8 %) | 2.2 (8 %) | 2.4 (10 %) | 1.6 (7 %) |
| $SO_4^{2-}$ | 2.8 (9 %) | 2.8 (11 %) | 2.7 (11 %) | 2.3 (11 %) |
| $NH_4^+$ | 0.9 (3 %) | 0.7 (3 %) | 0.7 (3 %) | 0.5 (2 %) |
| EC | 1.4 (5 %) | 0.9 (3 %) | 0.7 (3 %) | 0.5 (2 %) |
| OC | 4.2 | 2.5 | 2.5 | 2.3 |
| OM | 5.2 (17 %) | 4.2 (16 %) | 4.2 (17 %) | 4.6 (21 %) |
| Trace elements | 0.16 (0 %) | 0.16 (1 %) | 0.10 (0 %) | 0.10 (1 %) |
| Unaccounted | 9.8 (32 %) | 9.0 (35 %) | 7.8 (31 %) | 7.7 (35 %) |





ACPD
15, 33331–33378, 2015



**Table 2.** Mean concentrations ($\mu g\,m^{-3}$) of PMF factors at the Road Site (RS), Urban Background (UB), Torre Mapfre (TM) and Torre Collserola (TC).

| PMF Factors ($\mu g\,m^{-3}$) | RS | UB | TM | TC |
|---|---|---|---|---|
| Exhaust and wear | 8.7 (27 %) | 5.0 (18 %) | 2.9 (11 %) | 1.9 (10 %) |
| Road dust | 3.8 (12 %) | 3.3 (12 %) | 2.3 (9 %) | 1.6 (8 %) |
| Mineral | 4.6 (13 %) | 5.1 (18 %) | 4.8 (19 %) | 4.9 (26 %) |
| Aged marine | 4.6 (14 %) | 3.6 (13 %) | 5.2 (20 %) | 2.6 (13 %) |
| Heavy oil | 0.5 (2 %) | 0.6 (2 %) | 0.6 (2 %) | 0.4 (2 %) |
| Industrial | 1.2 (4 %) | 1.4 (5 %) | 0.7 (3 %) | 0.9 (5 %) |
| Sulphate | 3.5 (11 %) | 4.2 (15 %) | 3.8 (15 %) | 3.3 (17 %) |
| Nitrate | 5.7 (17 %) | 4.9 (17 %) | 5.5 (21 %) | 3.6 (19 %) |
| | 32.6 (100 %) | 28.1 (100 %) | 25.8 (100 %) | 19.2 (100 %) |





ACPD
15, 33331–33378, 2015



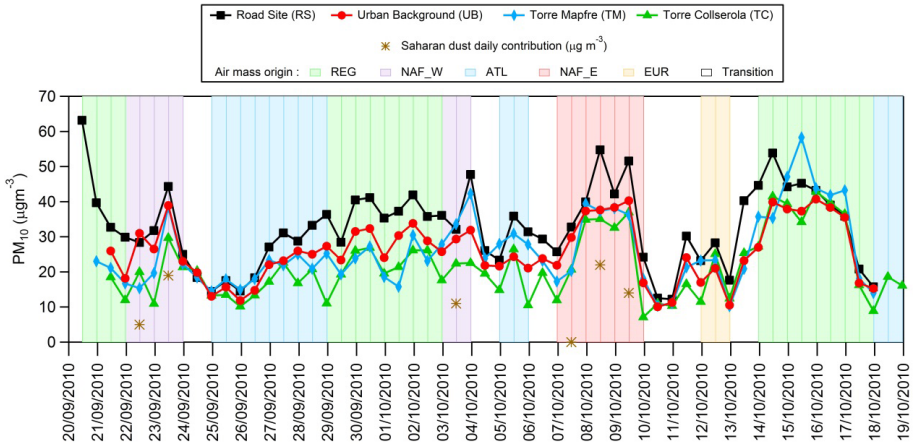


**Figure 1.** $PM_{10}$ variation at the 4 sites (RS, UB, TM, TC) during the SAPUSS campaign under different air mass origin (Regional (REG), North African West (NAF_W), Atlantic (ATL), North African East (NAF_E), European (EUR)). Saharan dust daily contribution to $PM_{10}$ is indicated.





ACPD
15, 33331–33378, 2015



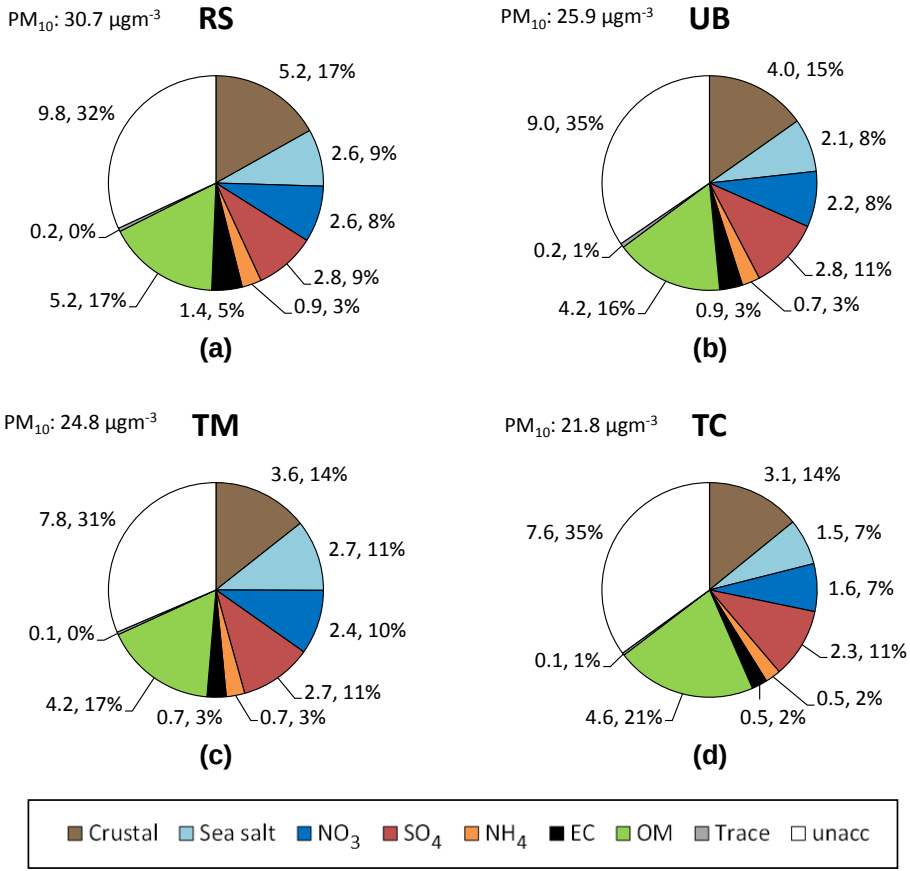


**Figure 2.** Mean composition of $PM_{10}$ concentration in $\mu g\,m^{-3}$ measured during the SAPUSS campaign at: **(a)** Road Site (RS), **(b)** Urban Background (UB), **(c)** Torre Mapfre (TM) and **(d)** Torre Collserola (TC). Data are given in $\mu g\,m^{-3}$ and %. On the top right of each graph average gravimetric $PM_{10}$ concentration are represented.





ACPD
15, 33331–33378, 2015



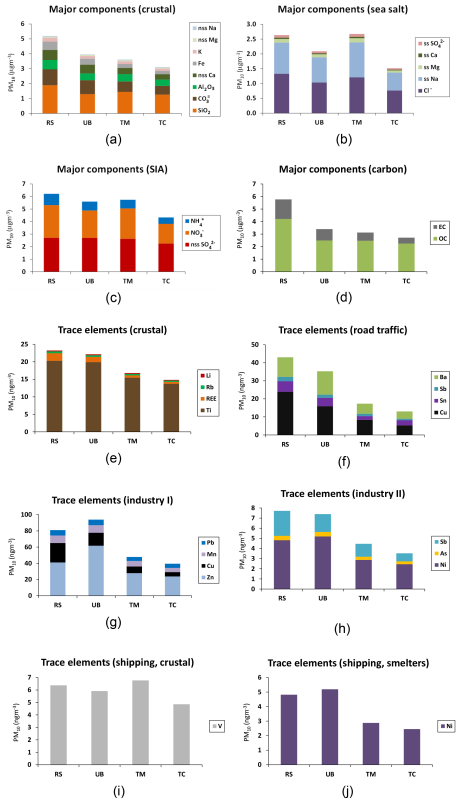


**Figure 3.** Average $PM_{10}$ concentration of main and trace elements for different emission sources at each site (RS: Road Site, UB: Urban Background, TM: Torre Mapfre, TC: Torre Collserola). REE denote Rare Earths elements.





ACPD
15, 33331–33378, 2015

Vertical and horizontal variability of $PM_{10}$ source contributions

M. Brines et al.



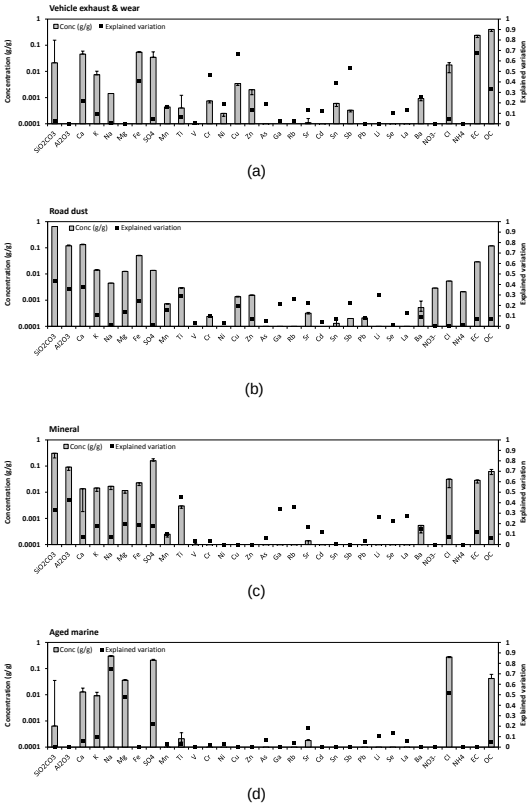


**Figure 4.**





ACPD
15, 33331–33378, 2015

Vertical and horizontal variability of $PM_{10}$ source contributions

M. Brines et al.



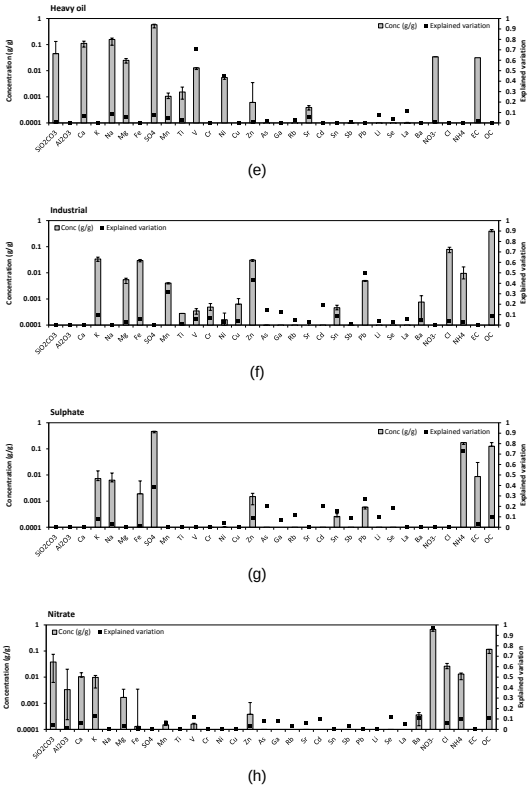


**Figure 4.** PMF sources profiles for $PM_{10}$ during the SAPUSS campaign: **(a)** vehicle exhaust and wear, **(b)** road dust, **(c)** mineral, **(d)** aged marine, **(e)** heavy oil, **(f)** industrial, **(g)** sulphate, **(h)** nitrate. Uncertainties were obtained by bootstrapping.





ACPD
15, 33331–33378, 2015



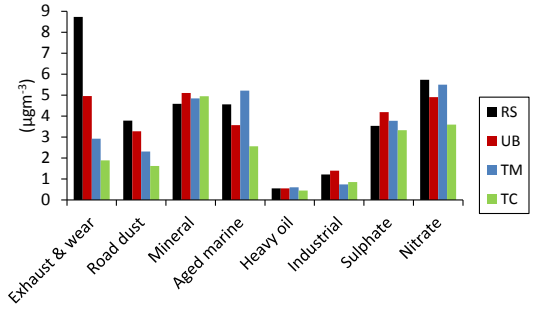


(a)

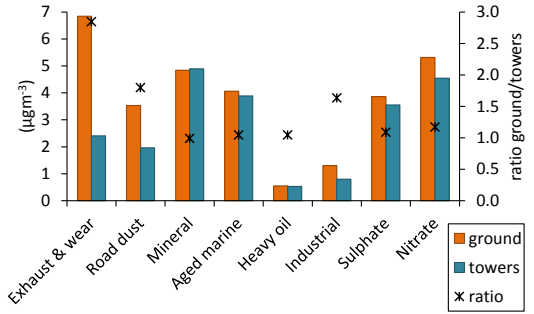


(b)

**Figure 5.** Contribution to $PM_{10}$ concentration levels of each of the eight factors: **(a)** at each of the 4 sites (RS, UB, TM, TC) and **(b)** at ground (RS and UB) and tower levels (TM and TC) and the concentration ratio between ground and tower sites during the SAPUSS campaign.





ACPD
15, 33331–33378, 2015



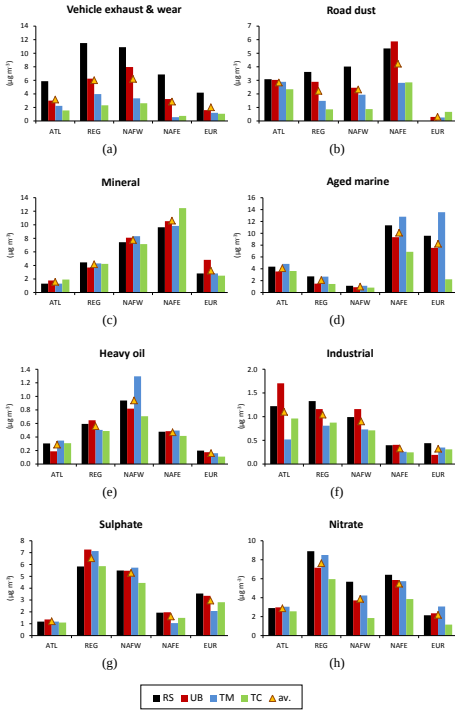


**Figure 6.** Average $PM_{10}$ contributions from the eight PMF factors at each of the sites (RS, UB, TM and TC) under different atmospheric scenarios (Atlantic, ATL; Regional, REG; North African West, NAFW; North African East, NAFE and European, EUR) during the SAPUSS campaign.





ACPD
15, 33331–33378, 2015



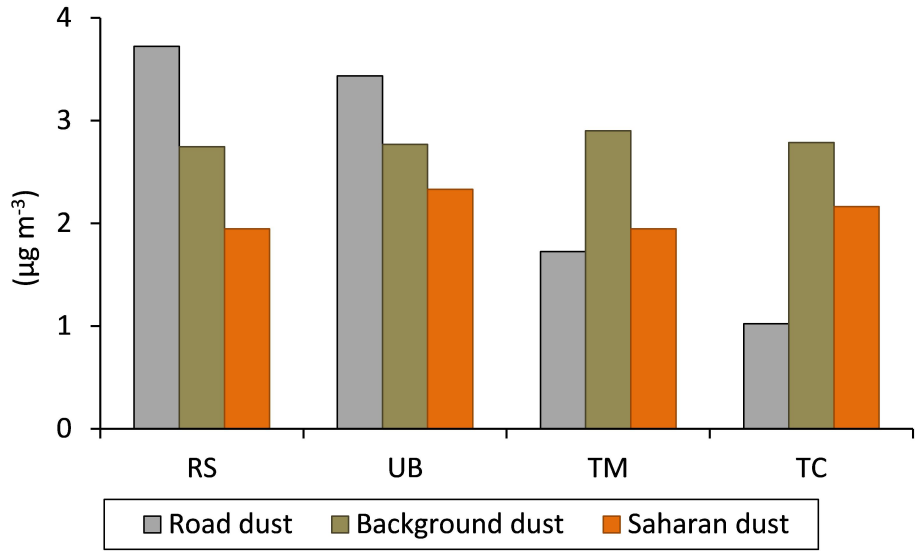


**Figure 7.** Average sources contributing to the mineral dust load during SAPUSS at the four monitoring sites RS, UB, TM and TC. Mineral background dust contributes on average 2.8 µg m$^{-3}$, road dust 2.7 µg m$^{-3}$ and Saharan dust 2.1 µg m$^{-3}$.





ACPD
15, 33331–33378, 2015



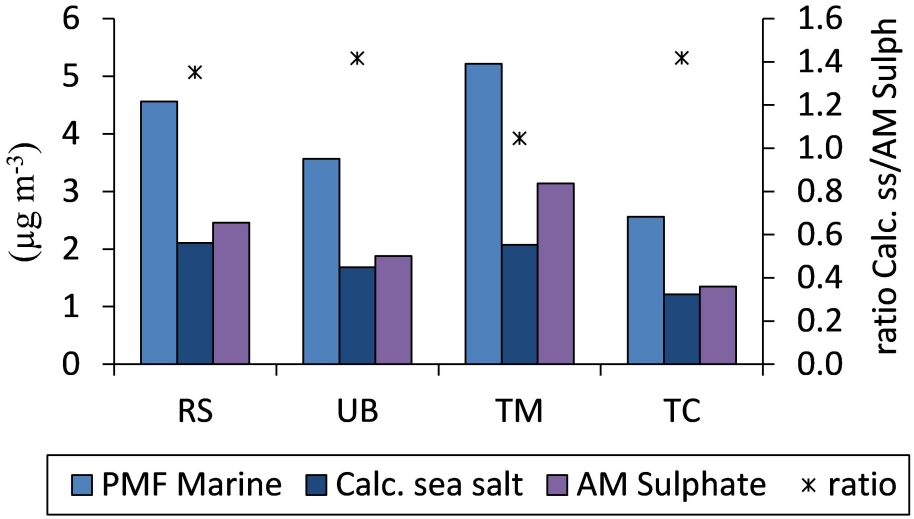


**Figure 8.** Average sources contributing to the sea salt factor during SAPUSS at the four monitoring sites RS, UB, TM and TC. Calculated sea salt contributes on average 1.8 µg m$^{-3}$ and marine sulphate from regional pollution 2.2 µg m$^{-3}$.





ACPD
15, 33331–33378, 2015



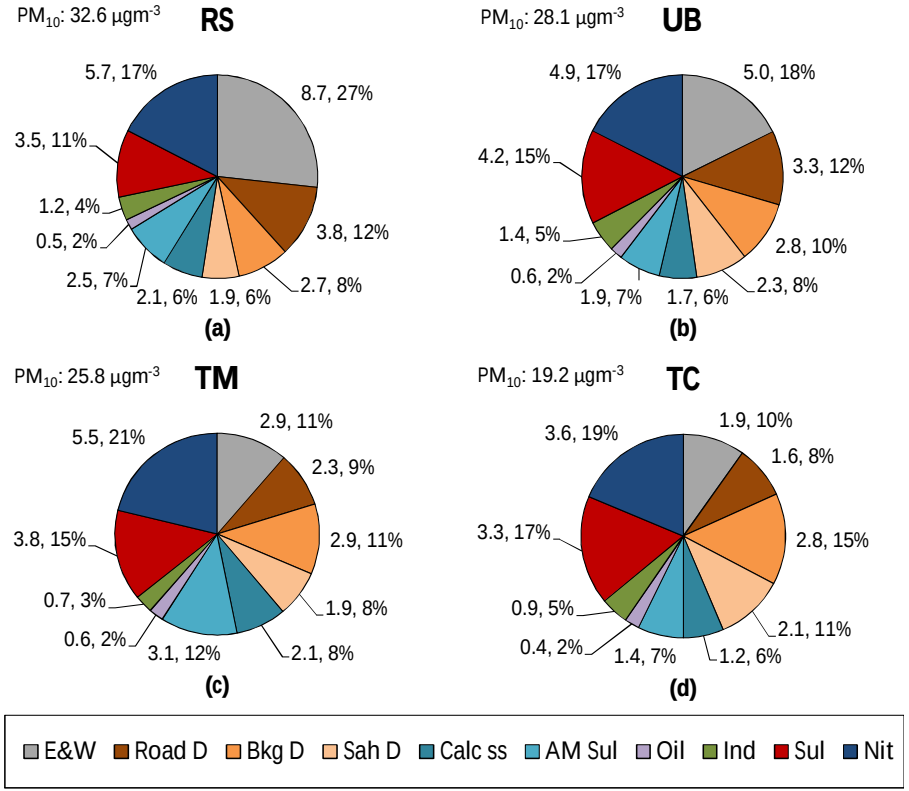


**Figure 9.** Sources contributing to the $PM_{10}$ load extracted with the PMF tool and subcomponents at each monitoring: **(a)** RS, **(b)** UB, **(c)** TM and **(d)** TC. Exhaust&Wear (E&W), Road dust (Road D), Heavy oil (Oil), Industrial (Ind), Sulphate (Sul) and Nitrate (Nit) are direct PMF factors. The mineral factor was broken into Background dust (Bkg D) and Saharan dust (Sah D) and the aged marine factor into Calculated sea salt (Calc ss) and Anthropogenic marine sulfate of regional origin (AM Sul). Data are given in $\mu g\,m^{-3}$ and %. The average PMF $PM_{10}$ concentration are represented at the top left of each graph for each site.





ACPD
15, 33331–33378, 2015